

Relativistic X-ray Lines from the Inner Accretion Disks Around Black Holes

*J. M. Miller*¹

¹Department of Astronomy and Astrophysics, The University of Michigan, 500 Church Street, Ann Arbor, Michigan, 48109, USA; email: jonmm@umich.edu

KEYWORDS: accretion physics, active galaxies, black holes, general relativity, X-ray astronomy, X-ray sources
X-ray astronomy

ABSTRACT: Relativistic X-ray emission lines from the inner accretion disk around black holes are reviewed. Recent observations with the *Chandra X-ray Observatory*, *X-ray Multi-Mirror Mission-Newton*, and *Suzaku* are revealing these lines to be good probes of strong gravitational effects. A number of important observational and theoretical developments are highlighted, including evidence of black hole spin and effects such as gravitational light bending, the detection of relativistic lines in stellar-mass black holes, and evidence of orbital-timescale line flux variability. In addition, the robustness of the relativistic disk lines against absorption, scattering, and continuum effects is discussed. Finally, prospects for improved measures of black hole spin and understanding the spin history of supermassive black holes in the context of black hole-galaxy co-evolution are presented. The best data and most rigorous results strongly suggest that relativistic X-ray disk lines can drive future explorations of General Relativity and disk physics.

CONTENTS

Introduction to Relativistic Disk Lines	2
<i>Initial Detections of Relativistic Disk Lines</i>	3
<i>Relativistic Lines and Disk Reflection: Theoretical Background</i>	4
Relativistic Disk Lines in Seyfert Active Galactic Nuclei	6
<i>Recent Studies of MCG-6-30-15</i>	6
<i>New Results from Well-Known Seyfert Active Galactic Nuclei</i>	7
<i>New XMM-Newton and Suzaku Surveys</i>	9
<i>Individual Carbon, Nitrogen, and Oxygen Lines</i>	10
<i>The Soft Excess in Seyfert-1 AGN</i>	11
Relativistic Lines from Disks Around Stellar-Mass Black Holes	12
<i>Lines Detected Prior to Chandra and XMM-Newton</i>	12
<i>The Chandra and XMM-Newton Era</i>	13
Line Variability – A New Frontier	14
<i>Relativistic Iron Line Flux Variations</i>	14
<i>Orbital-timescale Line Variations in Seyfert Active Galactic Nuclei</i>	16
<i>Orbital-timescale Line Variations in Stellar-Mass Black Holes</i>	17
Alternatives to Relativistic Lines and Dynamical Broadening	18

<i>The Effects of Warm-Absorber Disk Winds on Relativistic Lines</i>	18
<i>Scattering Effects and Broad Emission Lines</i>	19
An Informal Census of Relativistic Disk Lines	20
Constraints on the Innermost Accretion Flow Geometry	22
Summary and Future Prospects	23

1 Introduction to Relativistic Disk Lines

Accretion onto compact objects is the only viable means of powering the sustained X-ray energy release observed in active galactic nuclei (AGN) and in X-ray binaries. At sufficiently high fractions of the Eddington luminosity ($L_X/L_{Edd} \geq 0.001$, and perhaps also at smaller fractions), accretion onto both the supermassive black holes in AGN and stellar-mass black holes is thought to proceed through a standard Shakura–Sunyaev accretion disk (Shakura & Sunyaev 1973). As the inner disk can extend to within $6 GM/c^2$ of the black hole even in the absence of black hole spin, it may serve as a probe of the strong gravitational environment. In AGN, the innermost accretion disk spectrum peaks in the UV band; neutral hydrogen absorption can make direct measurements of the disk continuum very difficult. In stellar-mass black holes, the inner disk emits in X-rays with a typical temperature of $kT \simeq 1$ keV. In these cases, it is also difficult to get a clean measure of disk properties, due to strong Galactic line-of-sight absorption at low energy and simultaneous and overlapping hard X-ray emission. Moreover, in both AGN and stellar-mass black holes, the observational reality is that unambiguous signatures of gas orbiting close to a black hole – such as strong Doppler shifts and gravitational red-shifts – are not clearly revealed through continuum emission.

Owing only to a combination of abundance and fluorescence yield, Fe K-shell emission lines are the strongest X-ray emission lines in most AGN and X-ray binaries. When the disk ionization is low, fluorescence is the primary line emission mechanism; in highly ionized disks, recombination dominates. Inspired in part by the moderately broad Fe K line observed in the stellar-mass black hole Cygnus X-1 (Barr, White, & Page 1985), disk line models were calculated for two extreme cases: a zero-spin Schwarzschild black hole (Fabian et al. 1989), and a maximally-spinning Kerr black hole (Laor 1991). Both models predict a strongly asymmetric line profile with a red wing extending down to low energy. The Solid-state Imaging Spectrometer (SIS) aboard the *Advanced Satellite for Cosmology and Astrophysics* (or, *ASCA*) was the first X-ray spectrometer capable of revealing multiple X-ray lines from abundant elements. Moreover, the energy resolution of the SIS ($E/dE \simeq 30$, approximately) was sufficient to resolve the shape of X-ray lines. Observations with *ASCA* marked the true beginning of relativistic disk line studies.

In recent years, observations with *XMM-Newton* have led the way in detecting and measuring the properties of relativistic disk lines in Seyferts. While *Chandra* offers the highest spatial and spectral resolution and the lowest background, its low effective area means that it is less suited for relativistic disk line studies. The high effective area of *XMM-Newton* is essential: not only is the effective collecting area below the Fe K band higher than prior imaging missions, but so too is the effective collecting area above the Fe K band. While the lower energy

range is important for detecting the red wing of a relativistic line, the energy range above the line is essential for accurately measuring the continuum and disk reflection spectra. Moreover, accurately measuring the blue wing is essential for constraining the inner disk inclination. The high effective area and broad-band coverage of *Suzaku* (0.5–700 keV) position the observatory to make contributions to relativistic line studies that will equal or exceed even those of *XMM-Newton*.

In the sections that follow, recent detections and applications of relativistic accretion disk lines in the *Chandra*, *XMM-Newton*, and *Suzaku* era are discussed in the context of exploring general relativity and accretion onto black holes. The need to emphasize results which clearly demonstrate recent advances in the field imposes strong limits; some relevant studies are only mentioned in passing and others are omitted. Indeed, accretion onto black holes, accretion disks, the nature of spacetime close to black holes, and probes of strong gravitational effects are all large topics and deserving of more attention and explanation than is feasible herein.

Accretion onto black holes is treated thoroughly in Frank, King, & Raine (2002). Excellent general treatments of active galactic nuclei (AGN) are given by Peterson (1997) and Krolik (1999). Remillard & McClintock (2006) present a useful review of the phenomenology observed in stellar-mass black holes in X-ray binaries; this review and others are more complete and representative with regard to black hole spin diagnostics (see, e.g., Miller 2006). Relativistic disk lines are reviewed with specific attention to important theoretical aspects in Reynolds & Nowak (2003), and with attention to scattering processes and atomic transitions in Liedahl & Torres (2005). The reader is also referred to Fabian & Miniutti (2006) for a discussion of X-ray diagnostics of Kerr spacetime phenomena.

1.1 Initial Detections of Relativistic Disk Lines

Seyfert-1 AGN are the class of supermassive black holes that offer the cleanest view of the innermost accretion flow. As such, Seyfert-1 AGN are the optimal set of targets for relativistic disk line studies. Using the *ASCA*/SIS, Tanaka et al. (1995) first observed an asymmetric disk line profile in the Seyfert-1 AGN MCG-6-30-15. Other detections followed thereafter, and were greatly aided by the long-look observations made late in the *ASCA* mission. Systematic analysis of *ASCA* spectra of AGN are detailed in landmark survey papers by Nandra et al. (1997) and Reynolds (1997). Importantly, these surveys suggested that disk lines are common in Seyfert-1 AGN and should serve as a common diagnostic.

Photon counting rate limitations prevented the *ASCA*/SIS from making clear detections of relativistic disk lines in stellar-mass black holes. Despite its low spectral resolution, the gas imaging spectrometer (GIS) aboard *ASCA* could achieve detections of relativistic disk lines, but an observational emphasis on SIS spectroscopy served to ensure that few stellar-mass black holes were observed at high mass accretion rates. Indeed, although prior observations with gas spectrometers suggested the presence of disk lines in stellar-mass black holes, it was not until *Chandra* observed Cygnus X-1 that a single dynamically-broadened line was clearly revealed and separated from any narrow components (Miller et al. 2002a).

1.2 Relativistic Lines and Disk Reflection: Theoretical Background

In the case of white dwarfs, atmosphere models are a robust means of measuring the stellar surface gravity (see, e.g., Liebert et al. 2004). In accreting black hole systems, it is a combination of relativistic line and disk reflection models that is used to measure gravitational and Doppler shifts, and thereby inner disk radii and black hole spin. Physically and practically, modeling white dwarf atmospheres and black hole disk reflection are very similar. In both cases, the complex but entirely tractable details of gas processes and scattering are treated in order to accurately reveal gravitational effects.

A number of pure relativistic line models are available for spectral fitting through packages like XSPEC and ISIS (Arnaud 1996, Houck & Denicola 2000). The models are based on ray tracing: the Doppler shifts and gravitational redshifts imprinted on photons escaping from points close to a black hole are built-up in libraries. The most important considerations are the spin of the black hole, the radius of the inner edge of the accretion disk, the outer radius of line emission, the inclination at which the inner disk is viewed by a distant observer, and the line emissivity as a function of radius (r^{-3} is expected based on geometric considerations, assuming a standard thin accretion disk and isotropic source of disk irradiation).

In principle, lines emitted from the inner disk may be used to measure black hole spin because the innermost stable circular orbit (ISCO) around a black hole depends on the spin of a black hole: $r_{ISCO} = 6.0 r_g$ for $a = 0$, and $r_{ISCO} = 1.25 r_g$ for a maximal value of $a = 0.998$ (where $r_g = GM/c^2$ and $a = cJ/GM^2$; see Bardeen, Press, & Teukolsky 1972, and Thorne 1974). The line expected for an accretion disk orbiting a non-spinning Schwarzschild black hole was described by Fabian et al. (1989); the maximal spin Kerr case was described by Laor (1991). It was not until 2004 that models became available that included spin as a variable parameter that could be constrained directly by spectra. Such models have been developed and implemented into XSPEC by Dovciak, Karas, & Yaqoob (2004), Beckwith & Done (2004), and Brenneman & Reynolds (2006). The dependence of the ISCO on a and representative line profiles are shown in Figure 1. In the future, numerical simulations of standard thin accretion disks may be able to test analytic expectations for the dependence of an effective ISCO on a (present simulations can treat hot thick disks; see Krolik & Hawley 2002, Krolik, Hawley, & Hirose 2005).

In practice, black hole spin measurements with relativistic lines also depend on two principles that are upheld by observations and physically sound arguments. First, an accretion disk extends to the ISCO for a given value of a at all accretion rates above a certain threshold. Observations appear to strongly confirm this assumption. Second, gas within the ISCO emits only weakly. Theoretical arguments suggest that the gas within the ISCO should be hot, nearly fully ionized, and a negligible source of line emission (e.g. Young, Ross, & Fabian 1998; Brenneman & Reynolds 2006). Moreover, observed line profiles are very different than those predicted if line emission from within the ISCO is important (see, e.g., Reynolds & Begelman 1997).

Iron emission lines are the most obvious reaction of an accretion disk to irradiation by an external source of hard X-rays. The second important feature is an excess peaking between 20–30 keV due to Compton back-scattering; when added to power-law emission, this appears to be a flux excess that is sometimes called

the “reflection bump” (see the left panel in Figure 2). An external X-ray source is required because accretion disks do not efficiently self-irradiate; their emission peaks are well below the energy required to remove K-shell electrons from Fe atoms. The overall process of disk illumination and its response is known as disk reflection. The most important parameters in such models are the disk ionization state, the ratio of incident to reflected emission (equivalent to the “covering factor” in some models), the temperature of the disk, and the inclination at which the disk is viewed by a distant observer.

The reaction of a neutral disk to power-law irradiation is described by George & Fabian (1991). (An especially useful point of reference from this work is that reflection from a disk extending to the ISCO should produce an Fe K line with an equivalent width of 180 eV.) A power-law is typically assumed in such models because it is a reasonable representation of Comptonization, synchrotron, and/or synchrotron self-Comptonization spectra. Each of these processes might contribute to hard X-ray emission in black holes, in varying degrees. Since this initial study, a number of generalizations and refinements have followed (e.g. Ross, Fabian, & Young 1999; Nayakshin & Kallman 2001). These include the ability to handle high ionization parameters, the ability to account for different sources of hard X-ray irradiation, and different vertical density prescriptions (see the right panel in Figure 2). Most new reflection models explicitly include line emission (some intermediate models excluded the line components). Reflection models are calculated in the fluid frame, so they must be convolved with a relativistic line model in order to match the spectrum received by a distant observer. The parameters derived from fitting such a convolved spectrum can be used to constrain black hole spin; this procedure is merely a more complete method of deriving fundamental parameters than fitting the Fe disk line alone.

Many lines of evidence demand that hard X-ray emission in black hole systems be central and compact. The paradigm for many years was that hard X-rays originate via inverse-Compton scattering in a diffuse, hot corona. Many disk lines imply a centrally-concentrated source of hard X-ray emission; these findings and correlations between X-ray and radio (jet) fluxes imply that processes in the base of a jet (direct synchrotron and/or synchrotron self-Comptonization) may also be important. This suggests that the jet base may be only a few r_g in size, but this is broadly consistent with recent models (e.g. Markoff, Nowak, & Wilms 2005). However, the exact details do not need to be known for disk reflection to be modeled effectively: as long as a hard X-ray source illuminates the inner disk, reflection results, and iron lines can be exploited to measure fundamental quantities. Details of emission mechanisms aside, in practice the continuum X-ray emission in black holes is fairly simple. In Seyfert AGN, the continuum can be described with a simple power-law across the X-ray bandpass. In some cases, a “soft excess” is observed (see below); this component does not strongly affect the Fe K band. In stellar-mass black holes, both the disk and a non-thermal component can contribute in the soft X-ray band. However, these can be modeled effectively, and no continuum emission apart from a disk and power-law is statistically required in the strong majority of cases. With the addition of disk reflection and iron line components, stellar-mass black hole spectra are well-described, and strong lines are robust against different continuum models. Representative Seyfert-1 and stellar-mass black hole X-ray spectra are shown in Figure 3.

2 Relativistic Disk Lines in Seyfert Active Galactic Nuclei

2.1 Recent Studies of MCG-6-30-15

The Seyfert-1 AGN MCG-6-30-15 is presently the single most important source for studies of relativistic disk lines around black holes. Spectra from MCG-6-30-15 provided the first clear example of relativistic dynamics affecting the shape of a line (Tanaka et al. 1995), and new observations with *Chandra*, *XMM-Newton*, and *Suzaku* reveal strong evidence of black hole spin and possible signatures of gravitational light-bending. No other source has received the attention and scrutiny that MCG-6-30-15 has received. The strong line observed in its spectrum, and its relatively high broad-band X-ray flux, have served to ensure that it is a favorite target for observers. The same factors also make it an ideal test case for new disk line and reflection models. MCG-6-30-15 is, and will continue to be, the gold standard (however, devoting similar attention to other sources is essential for continued progress in the field).

The results of the first *XMM-Newton* observation of MCG-6-30-15 are presented in Wilms et al. (2001). The observation occurred in what may be called a “deep minimum” state (Iwasawa et al. 1996; see also Reynolds et al. 2004), wherein the disk line and reflection parameters are especially prominent relative to the continuum. Fits to the observed spectrum reveal an extremely skewed Fe disk line, with a red wing extending down to ~ 3 keV. The line was fit well using the Laor model with the inner radius extending down to $r_{in} = 1.23 r_g$ – strongly suggestive of a very high black hole spin parameter. This finding confirms prior evidence of spin initially revealed in especially long *ASCA* observations (Iwasawa et al. 1996). Importantly, fits to the iron line and reflection spectra in this initial *XMM-Newton* observation clearly require a steep line emissivity index ($q = 4.5$, recall $J(r) \propto r^{-q}$). If the hard X-ray source is an isotropic emitter, the steep emissivity profile is consistent with magnetic energy extraction from a spinning black hole dissipating extra energy in the inner accretion disk (Blandford & Znajek 1977; see also Agol & Krolik 2000).

Long-look observations of MCG-6-30-15 have provided precise measurements, and have proved to be important in establishing that the broad emission features observed can only be plausibly explained as emission lines shaped by relativistic effects (see Vaughan & Fabian 2004, A. K. Turner et al. 2004, and the discussion below). The results of a 320 ksec observation of MCG-6-30-15 are reported in Fabian et al. (2002). Here again, fits imply an extremely high spin parameter ($r_{in} = 2.0 \pm 0.2 r_g$) and enhanced inner energy dissipation ($q = 4.8 \pm 0.7$). Fabian et al. (2002) included fits with a broken power-law form for the line emissivity; at radii greater than $6 r_g$, the emissivity is consistent with expectations ($q = 3$). Whereas the fits made by Wilms et al. (2001) were based only on an *XMM-Newton* spectrum, the long-look observation detailed by Fabian et al. (2002) was made simultaneously with *BeppoSAX*, providing a continuum determination up to 100 keV. The broad-band spectrum also requires relativistically-skewed disk reflection. *Suzaku* observations of MCG-6-30-15 confirm results based on *XMM-Newton* data (see Figure 4), and demonstrate that explanations for line and continuum variability patterns that invoke gravitational light bending extend to the broad-band disk reflection continuum (Miniutti et al. 2007; more discussion of these results can be found below).

MCG-6-30-15 is the only black hole wherein a direct spin determination has

been made. This was achieved through fits with one of the new variable-spin relativistic line profiles noted above. Brenneman & Reynolds (2006) report $a = 0.989^{+0.009}_{-0.002}$ (90% confidence errors) based on fits to *XMM-Newton* spectra. This measurement is especially robust – a conservative continuum spectral model was used that allowed for the effects of absorption at low energy (for more on the effect of low energy absorption, see the sections below). The result is of obvious importance by itself, but it also demonstrates that fits with the maximal-spin Laor line model that yield small inner radii do indeed serve as strong indications of high spin (e.g. $a \geq 0.9$). It is interesting to note that the extremely high spin parameter suggested by these fits would rule out spin-down through magnetic field coupling; that possibility was suggested by Wilms et al. (2000) to account for the steep emissivity parameter required by the line.

Some studies have concluded that relativistic disk lines cannot serve as good indicators of black hole spin, because the nature of emission within the plunging region is uncertain and may serve to give faulty information on the ISCO (see, e.g., Dovciak et al. 2004). This conclusion appears to be largely incorrect. Sensitive spectra may indeed permit meaningful spin measurements. Gas within the plunging region is likely to be fully ionized, giving no line emission. Indeed, Brenneman & Reynolds (2006) constructed models forcing emission from within the plunging region, and these models give unphysical results when they are applied to the spectrum of MCG-6-30-15. It should also be noted that black hole spin is essential to models that succeed in describing disk line and continuum variability in black hole. To the extent that variability can serve as a check on spin measurements from direct line fitting, current variability studies suggest that direct line fitting is yielding accurate spin constraints (see, e.g., Miniutti & Fabian 2004).

2.2 New Results from Well-Known Seyfert Active Galactic Nuclei

NGC 3516: An analysis of initial *Chandra* and *XMM-Newton* spectra is presented in Turner et al. (2002). In addition to the clear detection of relativistic disk line profile like that found in MCG-6-30-15, the spectra appear to have *narrow* Fe line components. If the shifts of the narrow components is interpreted in terms of Doppler shifts, enhanced emission from $35 r_g$ and $175 r_g$ is implied; this may be consistent with warps or with hard X-ray emission arising in distinct co-rotating magnetic flares. The detection of distinct narrow features in this observation was the first observational realization of the potential of Fe K lines to trace orbital-timescale variability in Seyfert AGN. Subsequent studies have yielded important results that are discussed in more detail below. Fits to the relativistic disk line revealed in *Suzaku* observations are detailed in Markowitz et al. (2006).

NGC 4051: Initial observations of NGC 4051 with *Chandra* and *XMM-Newton* are reported in Uttley et al. (2003) and Uttley et al. (2004). Observations with *RXTE* were made simultaneously with *Chandra*, and a good fit is obtained when a Laor line is included in the full spectral model. Indeed, fits with the Laor component give $r_{in} = 1.33 r_g$, suggestive of a high black hole spin parameter. The *XMM-Newton* spectrum also shows evidence of a relativistic disk line, but it is not modeled explicitly in Uttley et al. (2004). Ogle et al. (2004) explicitly fit the relativistic line detected detected with *XMM-Newton* using a Laor model, and measure $r_{in} \leq 2.1 r_g$. This small inner radius is consistent with the line results reported by Uttley et al. (2003), and consistent with fits to a possible O VIII line in the *XMM-Newton* gratings spectrum (see below). Spectral variability analysis

by Ponti et al. (2006) also suggests a very small inner disk radius compatible with high spin.

Markarian 766: The first reports on *XMM-Newton* observations of Mrk 766 focused on putative relativistic C, N, and O disk lines (these features are discussed in a subsequent section). Mason et al. (2003) report on fits to the relativistic Fe line in Mrk 766 using the Laor model; an inner disk radius of $r_{in} = 1.32_{-0.1}^{+0.8}$ is measured, suggesting that Mrk 766 may also harbor a black hole with a high spin parameter. More recently, extremely deep observations of Mrk 766 with *XMM-Newton* have revealed evidence for orbital-timescale variability in narrow Fe line components (Turner et al. 2006).

MCG-5-23-15: *XMM-Newton* observations of the Seyfert 1.9 MCG-5-23-16 also reveal a relativistic disk line (Dewangan, Griffiths, & Schurch 2003; also see Balestra, Bianchi, & Matt 2004). It is unusual to observe relativistic disk lines in Seyfert-2 AGN because the torus prevents a clear view of the inner accretion disk. In MCG-5-23-16, the Fe K line profile implies an inclination of 47° – higher than that in sources like MCG-6-30-15 ($i \leq 30^\circ$). Though the line profile is clear, its shape is not as well determined as other relativistic iron lines, and there is no statistical distinction between line models assuming zero spin and maximal spin (Dewangan, Griffiths, & Schurch 2003; Reeves et al. 2007). Figure 5 and Figure 6 depict the *Suzaku* spectrum of MCG-5-23-16.

NGC 5548: In a few sources, indications for broad Fe K lines in *ASCA* spectra have not been confirmed with new observatories, and NGC 5548 is one example. Independent systematic analyses found evidence for broad Fe K emission lines in *ASCA* spectra of NGC 5548 (Reynolds 1997, Nandra et al. 1997). Pounds et al. (2003a) analyzed an *XMM-Newton* observation of NGC 5548, and report no evidence of a broad disk line (though an upper limit on such a feature is not given). The Fe K line emission is restricted to a single narrow line from neutral iron, consistent with reflection from the distant torus. If the disk line is truly absent, it is difficult to explain within the context of simple disk reflection geometries. However, sources that have been studied more extensively – such as MCG-6-30-15 – show strong variations in line strength and a saturation of the line at high continuum flux levels.

NGC 3783: Spectra of NGC 3783 obtained by *ASCA* provided some of the most compelling emission line profiles detected in that era (see, e.g., Nandra et al. 1997 and Reynolds 1997). Observations with *Chandra* and *XMM-Newton* have revealed that the low energy absorption in this Seyfert AGN is extremely complex, and may have an influence even up to the Fe K band (see Kaspi et al. 2002, Reeves et al. 2004, and Yaqoob et al. 2005). Fits to these new spectra demonstrate that distinguishing the red wing of a relativistic line from curvature due to low-energy absorption is difficult (but not impossible) when low-energy absorption is strong. Although NGC 3783 has a uniquely rich absorption spectrum, the realization that low-energy absorption can plausibly affect the Fe K band fueled attempts to explain relativistic disk lines in other sources as absorption-induced modeling artifacts. New individual observations and survey work makes it clear that relativistic lines are robust and required even when low-energy absorption is strong (Nandra et al. 2006; Reeves et al. 2006).

2.3 New XMM-Newton and Suzaku Surveys

Some initial analyses of Seyfert spectra obtained with *XMM-Newton* were complicated by uncertainties in the instrumental calibrations and background flux. Other work over-estimated the role of low-energy absorption in shaping the continuum in the Fe K band (again, see the discussion below). With the instrument characteristics and proper scope of low energy absorption better understood, Nandra et al. (2006) have undertaken a systematic analysis of Seyfert AGN spectra obtained with *XMM-Newton* (also see Guainazzi, Bianchi, & Dovciak 2006). This analysis is both rigorous and conservative: the spectral models are sophisticated and are in no way biased to detect relativistic disk lines. Apart from reasonable continua, the spectral models include variable low energy absorption, a narrow Gaussian emission line to account for distant emission from the torus, relativistic disk line models, and disk reflection. An especially important result of this work is that broad Fe lines consistent with a disk origin are detected in 73% of the sample of 30 objects; this is consistent with *ASCA* surveys despite the more conservative approach, and clearly demonstrates that disk lines are very common.

Nandra et al. (2006) measure relativistic disk lines that require emission from within $20 r_g$ in nine Seyferts, including: NGC 2992, MCG-5-23-16, NGC 3516, NGC 3783, NGC 4051, NGC 4151, Mrk 766, and MCG-6-30-15. In each of these cases, alternative explanations for the red wing of the lines, including low energy absorption shaping the continuum, are statistically rejected. The results reported by Nandra et al. (2006) differ slightly from others, in that only marginal evidence for black hole spin is found (in NGC 3783 and NGC 4151). This is likely because a specific prescription for the disk emissivity is enforced: $q = 0$ within a break radius, and $q = 3$ at greater radii. This choice does not affect the detection of relativistic disk lines, but it does serve to affect constraints on the inner disk radius and therefore black hole spin. Analyses that allow the data to determine the emissivity do find strong evidence of spin (e.g. Fabian et al. 2002, Brenneman & Reynolds 2006). As the field is still developing a picture of the corona and how it might illuminate the disk, allowing the data to decide is the best possible approach.

New observations of Seyfert AGN with *Suzaku* have also clearly revealed relativistic disk lines in a number of sources. *Suzaku* is uniquely able to cover an energy range extending an order of magnitude below and above the Fe K band. This means that the Compton back-scattering hump peaking between 20–30 keV cannot merely be detected, but rather it can be measured well. Detections of the reflection hump demand that the correct description of the spectrum must include a disk line and reflection. In an initial survey of seven Seyfert AGN, Reeves et al. (2006) report the detection of relativistic Fe disk lines and reflection in six sources: MCG-5-23-16, MCG-6-30-15, NGC 4051, NGC 3516, 3C 120, and NGC 2992. In one case, NGC 2110, there is no evidence of a relativistic disk line or reflection. This *Suzaku* detection fraction (86%) is thus broadly consistent with the *XMM-Newton* results reported by Nandra et al. (2006).

A few *Suzaku* results are particularly worthy of note. Spectra of NGC 3516 clearly reveal a relativistic disk line (the line is required at more than 99.999% confidence), despite relatively complex low-energy absorption and narrow emission components within the Fe K band (Markowitz et al. 2006; Reeves et al. 2006). Spectra of MCG-6-30-15 reveal relativistically-skewed disk reflection, consistent

with the relativistic iron line detected in *XMM-Newton* observations (Miniutti et al. 2007). Moreover, the *Suzaku* observations show that the disk reflection spectrum follows the same variability pattern as the iron line; not only does this tie these features together in the way anticipated theoretically, but it is additional evidence that gravitational light bending may drive much of the observed flux variability (see below). The same variability pattern is observed in *Suzaku* observations of NGC 4051 and MCG-5-23-16, further supporting this picture (Reeves et al. 2006, 2007; see also Ponti et al. 2006).

2.4 Individual Carbon, Nitrogen, and Oxygen Lines

As noted above, iron is merely the most prominent disk reflection line owing to a combination of its abundance, fluorescent yield, and ability to retain electrons at high temperature. For a plausible range of ionization parameters (up to $\xi = 10^3$, where $\xi = L/nr^2$; see, e.g., Ballantyne, Ross, & Fabian 2002), disk reflection models predict that relativistic O VIII disk lines should be visible as weak (30–70 eV in equivalent width, assuming solar metallicity) spectral features on top of the continuum. Detecting such lines in many Seyfert AGN is complicated by the presence of a warm absorber in soft X-rays. A fair assessment of present results is that there is evidence in favor of such lines, but no conclusive detections.

A major finding of the *ASCA* era was that many Seyfert-1 AGN have low-energy spectral complexity consistent with ionized absorption (Reynolds 1997). The spectra of these "warm absorbers" strongly suggests that O VII and O VIII contribute significantly to the total opacity. Higher resolution observations with the *Chandra*/HETGS and *XMM-Newton*/RGS have since confirmed this in many cases, and strongly suggest that warm absorbers are related to disk winds. In an analysis of the first *XMM-Newton*/RGS spectra of MCG-6-30-15 and Markarian 766, however, Branduardi-Raymont et al. (2001) proposed that the apparent edges seen in the spectra are actually the blue wing of relativistic C VI, N VII, and O VIII lines. This interpretation partially hinged on the finding that the O VII edge was either absent or red-shifted by 16,000 km/s; the latter was deemed unlikely as no O VII absorption lines were found to be similarly red-shifted. This emission line model does fit the strongest features in the soft X-ray bandpass well, and the small inner disk radii inferred ($r = 1.24 r_g$) are consistent with Fe K line results (Wilms et al. 2001; Fabian et al. 2002). However, this model alone does not account for a number of observed absorption lines.

An analysis of the initial *Chandra*/HETGS spectrum of MCG-6-30-15 found the O VII edge at its rest wavelength, and attributed the apparent red-shift of the edge in the *XMM-Newton* spectrum to a combination of O VII lines and Fe L absorption (Lee et al. 2001). The model adopted to describe the *Chandra* spectrum requires that some of the iron be embedded in dust within a highly ionized medium in order to match optical reddening. This "dusty warm absorber" model produced a good fit to the *Chandra*/HETGS spectrum without requiring strong relativistic C VI, N VII, or O VIII lines.

Although both initial spectra were of limited sensitivity and both models are physically motivated, the strong discrepancy between these interpretations sparked a vigorous debate. In fact, a combination of both models may give the best description of the data. A thorough re-analysis of the *XMM-Newton*/RGS spectra of MCG-6-30-15 and Markarian 766 by Sako et al. (2003) finds that relativistic lines still dominate, but that a combination of relativistic lines and a

dusty warm absorber is required. The relativistic O VIII disk line measured by Sako et al. (2003) has an equivalent width of 162 ± 8 eV; this is higher than predicted by disk reflection models (e.g., Ballantyne, Ross, & Fabian 2002). Ogle et al. (2004) report evidence for a relativistic O VIII line in *XMM-Newton* spectra of NGC 4051 with an equivalent width of ~ 90 eV, which is more consistent with current models.

At present, the definitive statement on the possibility of relativistic lines from elements other than iron likely comes from an analysis of the 320 ksec *XMM-Newton* long-look observation of MCG-6-30-15. A. K. Turner et al. (2004) find that the best-fit dusty warm absorber model leaves residuals consistent with relativistic lines, that the best-fit relativistic lines model requires dusty warm absorption, and that neither model (by itself) is a statistically superior description of the time-averaged spectrum. In a procedure borrowed from analysis of continuum versus iron K line variability, Turner et al. (2004) derive a high-flux minus low-flux difference spectrum to illustrate that absorption must be the dominant effect at low energy, and that relativistic lines (O VIII in particular) are constrained to have equivalent widths of approximately 30 eV or less (broadly consistent with theoretical expectations).

In summary, relativistic disk lines from elements such as carbon, nitrogen, and oxygen are predicted by disk reflection models, and it should be possible to detect them even though they are weak. By virtue of its (relatively high) energy, O VIII should be the most easily detected soft X-ray line within a typical X-ray CCD or X-ray calorimeter bandpass. The longest observations and most careful analyses provide some initial evidence for relativistic O VIII disk lines in cases where relativistic Fe K lines are clearly detected. Evidence for other lines is considerably weaker, especially after accounting for the effects of warm absorbers, which appear to be the dominant source of spectral complexity at low energy in Seyfert-1 AGN. Clearly detecting relativistic O VIII lines is just within the reach of *XMM-Newton* and *Suzaku*, and should be easily possible with planned missions such as *Constellation-X* and *XEUS*. Such lines will offer an important check on black hole spin measurements and results related to strong field effects such as gravitational light bending.

2.5 The Soft Excess in Seyfert-1 AGN

It has recently been realized that the “soft excess” flux observed in addition to a simple power-law continuum in some Seyfert-1 AGN (Arnaud et al. 1985) is not thermal flux arising from the accretion disk. Such soft flux components are especially common in “narrow-line” Seyfert-1 AGN, which are thought to harbor lower mass black holes than standard Seyfert-1 AGN. Not only are the temperatures inferred from blackbody fits to these components unreasonably high ($kT \simeq 0.1\text{--}0.2$ keV), but the temperatures do not vary with luminosity (e.g., Gierlinksi & Done 2004). This has recently led to attempts to describe the soft X-ray excess in terms of discrete atomic features.

The energetics and timescales observed from accretion onto compact objects demand that X-ray emission is extremely centrally-concentrated. As a result, matter at hundreds or thousands of Schwarzschild radii will see the central engine as a point source. (If the X-ray emission is strongly scattered in a large volume around the black hole, the point source approximation may be invalid; however, many spectroscopic and timing studies suggest that this is unlikely.) Therefore,

X-ray absorption is only sensitive to velocities directly along the line of sight connecting the central engine and the observer. Accreting matter tends to move perpendicular to this line of sight, unless it is being expelled in a wind. It is unlikely that the soft excess can be due to blurred absorption (e.g., Gierlinski & Done 2004), then, as encoding tangential velocities in absorption is extremely difficult, and a broad range of high velocities both toward and away from the observer along a single line of sight would be required to blur away individual absorption features.

Instead, the soft X-ray excess in some Seyfert-1 AGN may be due to a collection of blurred soft X-ray emission lines from the accretion disk (e.g., Ballantyne, Iwasawa, & Fabian 2001; Crummy et al. 2006). This requires a low ionization parameter so that many disk lines can be produced and blended together by relativistic blurring. Fits to a sample of Seyfert-1 AGN with a blurred disk reflection model for the soft excess suggest that near-maximal spin is preferred in the strong majority of cases (Crummy et al. 2006). This is broadly consistent with expectations (Volonteri et al. 2005), and may serve as a check on results based on Fe K lines. However, clear detections of more distinct low-energy lines (from more ionized disks) in the future would likely provide a favored complement to relativistic iron line results, as individual line features bear the hallmarks of relativistic shifts more clearly than blends which approximate a continuum.

3 Relativistic Lines from Disks Around Stellar-Mass Black Holes

3.1 Lines Detected Prior to *Chandra* and *XMM-Newton*

As noted previously, it was a broad Fe K emission line in the spectrum of the stellar-mass black hole X-ray binary Cygnus X-1 (Barr, White, & Page 1985) that incited much of the original theoretical work on relativistic disk lines and the subsequent observational studies of Seyfert galaxies. Until recently, however, studies of disk lines in stellar-mass black holes progressed more slowly than in the case of Seyfert AGN. An *EXOSAT* spectrum of 4U 1543–475 revealed a broad, asymmetric iron line (van der Woerd, White, & Kahn 1989; see also Park et al. 2004). Done & Zycki (1999) looked at many spectra of Cygnus X-1 and reported evidence of relativistic smearing in the broad-band reflection spectrum, not merely the Fe K emission line. Similar results were reported in V404 Cyg (Zycki, Done, & Smith 1999). Based on *RXTE* data, Balucinka-Church and Church (2000) reported the detection of an extremely broad Fe K emission line in spectra of the stellar-mass black hole GRO J1655–40, and Miller et al. (2001) reported a broad Fe K emission line in spectra of XTE J1748–288.

Although each of these results made progress, they were achieved using gas detectors with characteristic energy resolutions of ~ 5 (E/dE , or $0.2c$). Therefore, these results were less compelling than the detections and asymmetries seen in *ASCA* CCD spectra of Fe K lines in Seyfert AGN. Efforts to study the Fe K line in Cygnus X-1 using the *ASCA*/SIS were severely hampered by photon pile-up (pile-up is the result of two photons registering as one because they arrive within a single CCD frame time; see, e.g., Ebisawa et al. 1996).

The best studies of relativistic disk lines in stellar-mass black holes prior to studies with *Chandra* and *XMM-Newton* targeted GRS 1915+105 (Martocchia et al. 2002). Broad-band spectra obtained with *BeppoSAX* display prominent and skewed Fe K disk lines. Fits to these lines imply a truncated accretion

disk, thus offering no evidence of black hole spin. (These results are consistent with later observations made using *XMM-Newton*; see Martocchia et al. 2006.) An extremely high inner disk ionization may inhibit the detection of spin in GRS 1915+105. Taken at face value, however, these results call into question subsequent claims for maximal spin based on disk continuum fits (McClintock et al. 2006). It is worth noting again that disk continuum fits cannot unambiguously reveal gravitational shifts and Doppler shifts, and so must be regarded with caution.

3.2 The Chandra and XMM-Newton Era

Chandra and *XMM-Newton* have CCD spectrometers with fast clocking modes suited to observing sources with high fluxes, free of photon pile-up. This instrumental advance made it possible to clearly resolve broad iron lines in stellar-mass black holes, and to know that broad features seen at low resolution are indeed relativistic lines (rather than, e.g., a collection of narrow lines). A *Chandra*/HETGS observation of Cygnus X-1 clearly revealed a relativistic line in a stellar-mass black hole for the first time (Miller et al. 2002a). The line profile in Cygnus X-1 can be fit acceptably with a zero-spin line model (this is confirmed with *XMM-Newton*; see also Miller 2006), suggesting that this system may harbor a black hole with low or modest spin. This is broadly consistent with the expectation that accretion should drive-up spin; Cygnus X-1 is a young binary with an O9.7 Iab supergiant donor star.

An observation of XTE J1650–500 with *XMM-Newton* revealed an Fe K line that is extremely broad, and likely requires a very high spin parameter (Miller et al. 2002b). The line is well described by the maximal-spin Laor line profile, and fits require $r_{in} \leq 2r_g$. The line emissivity is found to be very steep, with $q \simeq 5$. Both of these parameters are similar to those measured in *XMM-Newton* and *Suzaku* observations of the Seyfert-1 AGN MCG-6-30-15 (Wilms et al. 2001; Fabian et al. 2002; Miniutti et al. 2007). The *XMM-Newton* measurements are confirmed and extended in an analysis of three *BeppoSAX* spectra of XTE J1650–500 (Miniutti, Fabian, & Miller 2004). Focusing only on the 2–10 keV portion of the *BeppoSAX* spectra, Done & Gierlinki (2006) note that a highly ionized wind could reduce the breadth of the line; however, this result is based on the low resolution spectra and a narrow bandpass, and is inconsistent with both the *XMM-Newton* results and the results of variability studies (Miniutti, Fabian, & Miller 2004; Rossi et al. 2005).

The recurrent transient GX 339–4 is to relativistic disk line studies in stellar-mass black holes as MCG-6-30-15 is to similar studies in Seyfert AGN. It has been observed on multiple occasions, at different fluxes, in different states, and with both *Chandra* and *XMM-Newton*. In all cases where the hard X-ray flux is prominent, a strong relativistic Fe K disk line is detected that is consistent with a high degree of black hole spin. Each relevant spectrum of GX 339–4 has been fit with both phenomenological continuum plus relativistic line models and more physically-motivated disk line plus reflection models. In each case, simultaneous observations with *RXTE* have been employed to define the broad-band continuum and overall disk reflection spectrum.

Chandra first observed GX 339–4 in outburst, while the source was in an “intermediate” state. Fits with the Laor relativistic line plus ionized disk reflection model give $r_{in} = 1.3_{-0.1}^{+1.7} r_g$ (Miller et al. 2004b). Similar fits to a 75 ksec obser-

vation of GX 339–4 in the “very high” and “low/hard” states give $r_{in} = 2 - 3 r_g$ and $r_{in} = 3.0 - 5.0 r_g$, respectively (Miller et al. 2004a, 2006a). The “very high” state spectrum is of particular interest, because the spectral and variability phenomena observed in this state most closely resemble the behavior seen in Seyfert AGN (please see Figure 7). Similar to the case of XTE J1650–500, the relativistic disk line seen in the very high state of GX 339–4 requires centrally–concentrated energy dissipation ($q = 5.5^{+0.5}_{-0.7}$).

An extremely skewed feature was recently reported in *XMM-Newton* spectra of GRO J1655–40, in which X-ray variability studies also find evidence for spin (see, e.g., Strohmayer 2001, Torok et al. 2005). In two observations, Diaz Trigo et al. (2006) report evidence for a relativistic line with $r_{in} = 1.4 - 1.5 r_g$. During the time that *XMM-Newton* made these observations, simultaneous observations with *RXTE* were made that are difficult to fit with standard broad-band reflection models. It is possible that different continuum modeling would serve to reduce the extremity of the measured line parameters.

The fact that relativistic disk lines are clearly revealed at moderate and high resolution gives confidence in prior results obtained with gas detectors. Many analyses using gas spectrometer data were soon to follow after the relativistic line in Cygnus X-1 was confirmed. Observations with *BeppoSAX* revealed broad iron lines in the black hole candidates 4U 1908+094 (in ’t Zand et al. 2002) and SAX J1711.6–3808 (in ’t Zand et al. 2002b). A review of archival *ASCA*/*GIS* data revealed relativistic disk lines in Cygnus X-1, GRO J1655–40, and GRS 1915+105, confirming prior results, and discovered a disk line in XTE J1550–564 (Miller et al. 2005). Please see Figure 8 for examples of lines found in archival data. Physically-motivated fits to these spectra with the Laor line model and “pexriv” reflection model (Magdziarz & Zdziarski 1995) measure $r_{in} = 1.6^{+4.0}_{-0.4}$ and $r_{in} = 1.8^{+0.5}_{-0.6}$ in XTE J1550–564 and GRO J1655–40, respectively. This suggests that XTE J1550–564 may harbor a rapidly spinning black hole, and strengthens existing evidence for high spin in GRO J1655–40. As with prior fits, there is no strong evidence for spin in GRS 1915+105 based on its relativistic disk line.

4 Line Variability – A New Frontier

4.1 Relativistic Iron Line Flux Variations

Multi-wavelength flux variability is seen in all accreting sources, and the fastest X-ray variability from black holes is expected to arise closest to the black hole itself. Because relativistic disk lines arise through illumination of the disk in this region, it is expected that variations in the relativistic iron line and reflection spectrum should always follow variations in the hard X-ray continuum in direct proportion. That is, relativistic iron line variations should follow variations in the continuum, and should show the same degree of variability. These expectations are most easily tested in Seyfert-1 AGN. In low flux phases, this expectation is borne out by observations. Yet, in higher flux phases, relativistic iron lines appear to be less variable than the continuum. The influence of gravitational light bending close to a spinning black hole provides an exciting explanation of this apparent discrepancy. Studies of line variability in stellar-mass black holes also affirm that broad iron disk lines arise very close to the black hole.

Sensitive new data and clever analysis techniques reveal that in low continuum

flux states, broad iron lines vary with the continuum flux in the manner predicted by simple reflection models. Vaughan & Fabian (2004) and Ponti et al. (2004) employed *XMM-Newton* observations and rms variability spectra to show that the red wing of the iron line is more variable than the local continuum when MCG-6-30-15 is in low flux phases (see also Reynolds et al. 2004). Indeed, these findings also serve to confirm the expectation that the narrow core seen in some relativistic line profiles either originates in the outer disk or torus (for a recent discussion, see Nandra 2006); the narrow line core is less variable than the local continuum.

Although the red wing of iron disk lines is more variable in low flux phases, rms variability spectra show the opposite trend in periods of relatively high flux. Indeed, although the relativistic line profile is clearly variable in time-selected spectra, the variability appears to be driven more by variations in the power-law continuum than by the line itself (e.g., Vaughan & Fabian 2004). In a prior analysis of a long *ASCA* observation of MCG-6-30-15, Shih, Iwaswa, & Fabian (2002) had also found that the relativistic iron line appears to be less variable than the continuum. As noted above, appeals to complex and/or variable absorption models cannot reconcile the apparently disjoint variability behaviors in low and high flux phases: flux-selected spectra show no evidence of progressive partial covering (Vaughan & Fabian 2004), and 47 of 51 absorption lines seen with *XMM-Newton* do not vary between high and low flux states (A. K. Turner et al. 2004). Evidence that absorption is not driving the variability is bolstered by new results from *Suzaku* observations of MCG-6-30-15 which reveal that the entire disk reflection spectrum up to 45 keV (where photoelectric absorption is unimportant) is less variable than the continuum (Miniutti et al. 2007).

Apparently disjoint disk line and continuum flux correlations can be explained with natural modifications that reflect the emerging prevalence of black hole spin and evolving ideas concerning the nature of the hard X-ray corona. The extended red wings in some relativistic disk lines signal black hole spin, and the effects of gravitational light bending are especially strong near to spinning black holes. Light bending is largely ignored in simple disk reflection models, but it is important because light bending can strongly affect the flux that the disk and a distant observer will receive from a constant-luminosity source (a magnetic flare above the disk, the base of a jet, etc.). Flux variability is often assumed to be due to a source with varying intrinsic luminosity but static size and distance from the black hole – but this is only assumption.

New studies show that gravitational light bending can account for the changing disk line and continuum flux patterns observed in a growing number of black holes, including: MCG-6-30-15 (Miniutti et al. 2003; Miniutti & Fabian 2004), NGC 4051 (Ponti et al. 2006; see also Reeves et al. 2006), 1H 0707-495 (Fabian et al. 2004), 1H 0419-577 (Fabian et al. 2005), MCG-5-23-16 (Reeves et al. 2006), and in the stellar-mass black hole XTE J1650-500 (Miniutti, Fabian, & Miller 2004; Rossi et al. 2005). More examples are likely to be revealed through analysis of new and existing *XMM-Newton* and *Suzaku* observations. Within the context of the light bending model, line and continuum fluxes are positively correlated when the illuminating X-ray source is within $\simeq 4 r_g$ of the black hole, weakly correlated or uncorrelated when the illuminating source is within 4–13 r_g , and uncorrelated or anti-correlated for greater source heights. A centrally-concentrated corona, consistent with the base of a jet or corotating magnetic flares above the disk, is a secondary but important implication of this model (flares and the base of a

jet may be the same thing, of course). The success of this model is extremely suggestive, not only of the importance of light bending, but of the nature of the corona as well. These results require a centrally-concentrated corona, consistent with the base of a jet or co-rotating magnetic flares above the disk (flares and the base of a jet may be aspects of the same thing, of course). Figure 9 illustrates the effects of gravitational light bending, and Figure 10 shows evidence for light bending in NGC 4051 and XTE J1650–500.

It does not appear likely that more careful treatment of e.g. the disk ionization state would explain these observations without invoking light bending, but more work is needed. More examples of variability consistent with light bending are likely to be revealed through analysis of new and existing *XMM-Newton* and *Suzaku* observations. Importantly, the proximity of hard X-ray emission close to the black hole implied by these and other results suggests that reverberation mapping with *Constellation-X* and/or *XEUS* is likely to be a highly successful probe of General Relativity.

4.2 Orbital-timescale Line Variations in Seyfert Active Galactic Nuclei

The next generation of major X-ray missions (*Constellation-X*, *XEUS*) will have the collecting area and energy resolution required to reveal the ISCO around supermassive black holes in unprecedented detail using Fe K line variability studies. This will enable scientists to better explore the predictions of General Relativity near to black holes, in part via reverberation mapping (see below) studies. The *XMM-Newton* and *Suzaku* X-ray observatories have the collecting area and sensitivity needed to provide early indications of orbital-timescale variability and evidence for orbiting "hot-spots" or disk turbulence, as shown in recent observations.

The first evidence for narrow and variable Doppler-shifted lines in the X-ray spectra of NGC 3516 and Mrk 766 was found by Turner et al. (2002) and Turner, Reeves, & Kraemer (2004). These narrow line components are consistent with the transient shifts expected when a disk reacts to an illuminating flare, or may indicate that certain radii close to the black hole are illuminated preferentially. Other examples of such lines have recently been detected with *XMM-Newton* and *Chandra* (see, e.g., Guainazzi 2003; Yaqoob et al. 2003; Dovciak et al. 2004; Iwasawa et al. 2004). It should be noted that in all cases, the narrow red-shifted lines are relatively weak, and do not contribute significantly to a relativistic line profile.

The most compelling case for orbital-timescale variability in narrow red-shifted Fe K lines is found in an analysis of *XMM-Newton* spectra of NGC 3516 presented by Iwasawa, Miniutti, & Fabian (2004). After the flux of the (relatively stable) relativistic emission line is modeled and subtracted, nearly four 25 ksec cycles of a line component moving between 5.7 keV and 6.5 keV are observed. The variability pattern revealed in a flux excess versus time map has a distinctive sawtooth pattern, which is consistent with Doppler shifts and gravitational red-shifts acting on orbits close to the black hole. The cycles are consistent with emission between 7–16 r_g , either due to a co-rotating (magnetic) flare or turbulence in the accretion disk (Iwasawa, Miniutti, & Fabian 2004; Armitage & Reynolds 2003). It should be noted that the observed variability implies a black hole mass of $(1-5) \times 10^7 M_\odot$, in agreement with reverberation mapping results (Onken et al. 2003). The observed variations are found to be significant at the 97% level of confidence

through extensive Monte Carlo simulations; this estimate is conservative because the probability of cyclic variability is very low. The cyclic variations detected in NGC 3516 are shown in Figure 11.

Cyclic variations in narrow Fe K lines may also be present in *XMM-Newton* observations of Markarian 766 (Turner et al. 2006). The flux excess versus time map is considerably more complex and noisy than that found in NGC 3516. The strongest variation seen corresponds to a period of 165 ksec, or a radius of approximately $115 r_g$ for a black hole mass of $4.3 \times 10^6 M_\odot$ (Turner et al. 2006; Wang & Lu 2001). This is partially at odds with a growing body of evidence (including relativistic line studies) that disk irradiation in black holes is strongly concentrated in the very innermost regions. The evidence for orbital variations in Markarian 766 is less compelling than that in NGC 3516, but serves to illustrate the potential power of such investigations.

4.3 Orbital-timescale Line Variations in Stellar-Mass Black Holes

Quasi-periodic oscillations (QPOs) are common features in the power spectra of accreting stellar-mass black holes and neutron stars (for a review, see van der Klis 2006). So-called "kHz" QPOs in millisecond X-ray pulsars are closely tied to the neutron star pulsation (spin) frequency, and the highest frequency oscillations in stellar-mass black holes (e.g., 100–450 Hz) are commensurate with Keplerian orbital frequencies at the ISCO. These facts signal that QPOs are very likely disk frequencies, regardless of whether a given QPO represents an orbital, precession, or resonance frequency. Lower frequency QPOs (somewhat arbitrarily, 10 Hz and below) are more common and can be much stronger than high frequency QPOs. If they are Keplerian frequencies, slower QPOs relate to radii as large as a few hundred r_g ; however, the energy dependence of these X-ray QPOs argues strongly that they arise closer to the compact object and thus represent super-orbital frequencies.

In some low-flux states, GRS 1915+105 displays exceptionally strong (10% rms, and higher) and stable low-frequency QPOs. Miller and Homan (2005) exploited the stability of strong 1 Hz and 2 Hz QPOs (found in separate observations) to extract phase-selected spectra, and find that the broad Fe K emission line in GRS 1915+105 varies with QPO phase. This result employed both direct spectral fitting and difference spectra, the latter demonstrating the line variability in a model-independent way. If these QPOs only represent Keplerian frequencies, the phase-dependence of the lines signals that they likely originate from within $170 \pm 50 r_g$ and $100 \pm 30 r_g$ (respectively). At these radii, relativistic shaping of lines is *inevitable*. The phase dependence observed is consistent with a warp or precessing ring in the inner disk, and may even be a signature of Lense-Thirring precession (see Markovic & Lamb 1998; Fragile, Miller, & Vandernoot 2005; Schnittman, Homan, & Miller 2006). This result builds on prior work which clearly demonstrated that Fe K lines are sensitive to variability frequencies (see, e.g., Gilfanov, Churazov, & Revnivtsev 2000); though prior efforts did not use QPOs or averaged over phase.

The result linking Fe K lines and QPOs is notable for a few reasons. First, it shows that Fe K lines must originate in the inner disk and be shaped by relativistic effects in a model-independent way. Second, this connection provides a unique way of mapping the inner accretion disk around stellar-mass black holes and neutron stars. Third – and perhaps most importantly – this result is analogous

to detections of orbital-timescale line variability in Seyfert-1 AGN such as NGC 3516 (Iwasawa, Miniutti, & Fabian 2004) in that it is becoming possible to explore inner disk structures, not just relativity, with Fe K emission lines. Future X-ray missions such as *Constellation-X* and *XEUS* will be able to exploit the Fe K–QPO connection to map inner disk structures and explore relativistic effects in a much greater number of systems.

5 Alternatives to Relativistic Lines and Dynamical Broadening

5.1 The Effects of Warm-Absorber Disk Winds on Relativistic Lines

As noted previously, whereas O VII and O VIII edges were sufficient to describe most of the "warm absorbers" detected in some Seyfert-1 AGN with *ASCA* (Reynolds 1997), the dispersive high-resolution spectrometers aboard *Chandra* and *XMM-Newton* revealed complex spectra rich in absorption lines and edges. This realization led to some charged claims that the red wing of relativistic Fe K lines might generally be the result of poor fits to curvature induced by low-energy absorption. The initial claims were largely restricted to conferences and were never published as actual fits to data in a journal paper (they are partially summarized a Ph.D. thesis; see Kinkhabwala 2003). However, a few scientists later explored this possibility in formal papers. After careful analysis of deep observations, and with added continuum constraints from *Suzaku*, it is clear that curvature in the Fe K band is properly attributed to the red wing of relativistic lines.

The Seyfert-1 galaxy NGC 3516 is an excellent case study. *ASCA* spectra revealed a notable relativistic line with a prominent red wing (see, e.g., Nandra et al. 1997; Reynolds 1997). An initial analysis of observations with *Chandra* and *XMM-Newton* confirmed the disk line, and also revealed evidence for variable narrow emission lines that may be related to orbital motions (Turner et al. 2002). In a later analysis of the *Chandra*/HETGS spectrum, it was found that a warm/hot absorber capable of creating curvature in the Fe K band was statistically permissible (Turner et al. 2005). In fact, if one looks closely at Figure 6 in Turner et al. (2005), it is clear that this model greatly over-predicts the observed absorption in the Fe K band (see Figure 12). The absorption model does not fit the data, strongly suggesting the observed curvature above 3 keV in NGC 3516 is actually due to the red wing of a relativistic line. The broad-band continuum is defined better in *Suzaku* observations of NGC 3516, leaving less uncertainty in the low energy spectrum. A relativistic disk line is required in the initial *Suzaku* spectrum at the 99.999% level of confidence, even when low-energy absorption from a warm absorber is included (Markowitz et al. 2006).

A careful analysis of a 522 ksec *Chandra*/HETGS spectrum of MCG-6-30-15 also rules out absorption creating or affecting the red wing; such absorption models predict a strong line in the Fe K band that is not observed (Young et al. 2005). Please see Figure 13 to see how absorption fails to fit the observed spectrum. This careful study follows from a thorough analysis of the 320 ksec *XMM-Newton* spectrum of MCG-6-30-15. Vaughan & Fabian (2004) conducted an extremely rigorous and broad-ranging analysis which examined many possible ways a line-like feature might arise (including absorption), and conclude that the relativistic line in MCG-6-30-15 is robust. This paper is recommended to the reader as perhaps the most complete paper on the topic, and an excellent

example of a rigorous analysis.

The most extreme example of complex low-energy absorption in a Seyfert-1 galaxy is likely NGC 3783. In an analysis of a 900 ksec *Chandra*/HETGS spectrum, Kaspi et al. (2002) report the detection of a Compton edge in the narrow component of the Fe K line, but do not consider a global spectral model appropriate for broad line studies. In an analysis of a deep *XMM-Newton* spectrum, Reeves et al. (2004) find that absorption may affect the Fe K range; this agrees with an analysis of the long *Chandra* exposure by Yaqoob et al. (2005) which only finds strong evidence for a small red extent to the Fe K line.

Even in the extreme case of NGC 3783, however, when absorption and relativistic disk line components are both included in spectral models and the data alone decide the relative importance of these features, a relativistic disk line is strongly required (Nandra et al. 2006). Indeed, as noted above, the recent and *systematic* effort to fit only the absorption strongly required by individual spectra finds that relativistic lines are required in the *XMM-Newton* spectra of NGC 2992, MCG-5-23-16, NGC 3516, NGC 3783, NGC 4051, NGC 4151, Markarian 766, and MCG-6-30-15 (Nandra et al. 2006). This demonstrates that even on a narrow energy band, a rigorous fitting procedure clearly reveals relativistic lines. The veracity of disk lines is even more strongly demonstrated in recent *Suzaku* observations, which clearly reveal relativistic lines above and beyond any absorption concerns in NGC 4051, NGC 2110, and 3C 120 (Reeves et al. 2006), NGC 2992 (Reeves et al. 2007, Yaqoob et al. 2007), MCG-5-23-16 (Reeves et al. 2006, Reeves et al. 2007), NGC 3516 (Reeves et al. 2007, Markowitz et al. 2007), and MCG-6-30-15 (Reeves et al. 2006, Miniutti et al. 2007).

Somewhat separate from the issue of modeling time-averaged spectra, it has recently been found that relativistic iron lines are more prominent in low flux states than in high flux states (see, e.g., Vaughan & Fabian 2004). This behavior is superficially consistent with variable absorption affecting the spectrum. If the apparent prominence of disk lines at low flux is actually caused by absorption, however, variability should be seen in discrete absorption features. In an analysis of the absorption lines in the 320 ksec *XMM-Newton* spectrum of MCG-6-30-15, A. K. Turner et al. (2004) find that only 4 of 51 absorption lines are variable. This dramatic *lack* of absorption variability strongly suggests that the observed spectral curvature is due to a relativistic disk line and broad-band disk reflection spectrum.

5.2 Scattering Effects and Broad Emission Lines

It has sometimes been argued that the breadth of Fe K lines is not caused by a combination of Doppler shifts and gravitational red-shifts in the inner disk, but due to Comptonization (e.g., Misra & Kembhavi 1998, Misra & Sutaria 1999). It has also been suggested that the red wing of Fe K lines might be due to relativistic ($v/c \simeq 0.3$), optically-thick, wide-angle or quasi-spherical outflows (see, e.g., Titarchuk, Kazanas, & Becker 2003; Laming & Titarchuk 2004; Laurent & Titarchuk 2007). In both cases, a preponderance of observational evidence and sound physical arguments rule-out these possibilities, and demand that broad lines are shaped primarily by dynamics.

The case of Compton broadening of the line in MCG-6-30-15 as described in the models of Misra & Kembhavi (1998) and Misra & Sutaria (1999) is treated in detail in Reynolds & Wilms (2000) and Ruszkowski et al. (2000). To cre-

ate a red wing, line photons must be primarily down-scattered, necessitating a Comptonization region around the central engine with $\tau = 4$ and $kT \leq 0.5$ keV. Several sound arguments rule-out this possibility: (a) the spectral break expected at $E_{br} = m_e c^2 / \tau^2 \simeq 30\text{--}40$ keV (Guainazzi et al. 1999) is not observed; (b) variability is observed corresponding to length scales too short to be observed given the optical depth; and (c) the (unobserved) blackbody component required to sustain the Compton region would violate the blackbody limit for reasonable size scales of the Comptonization region. Turner et al. (2002) have also pointed out that the detection of narrow features within the broad line in NGC 3516 argues against strong Comptonization. The same argument can be extended to any source with evidence for variable narrow emission lines, such as Mrk 766 (Turner et al. 2006).

The possibility of scattering creating red wings as per the models of Titarchuk, Kazanas, & Becker (2003), Laming & Titarchuk (2004), and Laurent & Titarchuk (2007) is discussed briefly in Miller et al. (2004a), but numerous other studies also bear directly on such models. Many observations clearly reveal X-ray flux variability on timescales corresponding to the innermost stable circular orbit around black holes, which is inconsistent with this region being screened by an optically-thick outflow. The predictions of simple reflection models are strongly confirmed in low continuum flux phases, and where the line flux does not trace the continuum flux, observations show that absorption and scattering cannot be the explanation. For examples, please see, e.g., Gilfanov, Churazov, & Revnivtsev 2000; Miniutti & Fabian 2004; Reynolds et al. 2004; Ponti et al. 2004; Vaughan & Fabian 2004; Iwasawa, Miniutti, & Fabian 2004; Miller et al. 2004a; and Miller & Homan 2005. Moreover, to achieve the degree of scattering required to produce the red wings observed in Fe K line spectra, highly super-Eddington outflows (as much as 10 times the Eddington rate) are required. The outflows implied in stellar mass black holes such as GX 339–4 are generally a small fraction of the Eddington mass accretion rate (Miller et al. 2004b, 2006b), and those seen in all black hole spectra fall well-below the velocity required ($v/c \geq 0.3$) for such effects to be important.

6 An Informal Census of Relativistic Disk Lines

The aim of this section is to collect an up-to-date census of sources with relativistic disk line detections. Evidence of C, N, and O disk lines is only reported in sources that have compelling Fe disk lines, so it is only necessary to count Fe lines. Reported lines with $\text{FWHM} \leq 0.1c$ are not considered, in order to ensure disk-like velocities. Similarly, detections of single *narrow* red or blue-shifted lines are not considered as they may be related to jet ejection events rather than disks. All of the stellar-mass black hole sources in the Remillard & McClintock (2006) catalog are considered; black hole “candidates” are not separated from dynamically-constrained systems because the phenomena observed in “candidate” sources strongly suggests black holes. The survey undertaken by Nandra et al. (2006) considered only Seyfert AGN with more than 100,000 X-ray photons detected with *XMM-Newton*, and made new spectral fits. The exposure threshold and uniformity of the Nandra et al. (2006) survey ensure that its estimate of the fraction of AGN with a broad disk line is robust. In contrast, the census undertaken here does not place a limit on how well a source has been observed,

and relies on fits reported in the literature. However, the list generated here is broad and may be a useful starting point for deeper observations and new studies.

As discussed at length above, the best examples of relativistic disk lines represent extremely incisive probes of black hole spin and the strong gravitational environment close to a black hole. The power of the the best detections is greatest, though, when we remain critical of all detections. In this spirit, reported disk lines have been divided into three groups: Tier 1, Tier 2, and Tier 3, from the most robust and incisive lines to those detected with less certainty. Because it is practical to do so, significant non-detections in stellar-mass black holes are also listed. The standards used to distinguish these groups cannot be exclusively quantitative because different scientists have employed different models, different instruments, and different statistical methodology. Moreover, the standards applied to lines from disks around stellar-mass black holes and disks in Seyfert AGN differ because of their intrinsically different low energy spectra, fluxes, and timescales. The criteria below describe the lines in each tier:

Seyfert AGN, Tier 1: Strong lines revealed in deep *Chandra* and/or *XMM-Newton* and/or *Suzaku* observations that are robust against plausible absorption and reveal possible evidence of black hole spin.

Seyfert AGN, Tier 2: Lines seen with *XMM-Newton*, *Suzaku*, or with *BeppoSAX* in shorter observations than sources in Tier 1. Line asymmetry may be less clear than Tier 1.

Seyfert AGN, Tier 3: Weak line detections, whether due to intrinsic weakness or very short observations.

Stellar-mass black holes, Tier 1: Lines detected with multiple instruments (if not an instrument with at least CCD spectral resolution, then an imaging mission with low energy coverage and a mission with broad energy range) and in multiple states with a clear asymmetric profile.

Stellar-mass black holes, Tier 2: Lines detected with multiple instruments, and/or in multiple states, and with an imaging mission with low energy coverage.

Stellar-mass black holes, Tier 3: Lines detected with *RXTE* only. Sources observed only with *Ginga* are not included.

Significant non-detections: Sources observed with a recent soft X-ray spectrometer covering the Fe K band, observed in states with strong hard flux, fit with now-standard continuum models, and in which observations can rule-out broad lines with an equivalent width of 180 eV (as per unity disk covering factor, George & Fabian 1991).

Analysis by Nandra et al. (1997) found disk lines in 77% of Seyfert-1 AGN observed with *ASCA*. Moreover, this work reported a strong disk line profile in the average spectrum of Seyfert AGN after excluding clear individual detections, further suggesting that such lines are common. The absence of strong detections in short initial observations with *Chandra* and *XMM-Newton* generated some concern about the veracity of lines detected with *ASCA*. Thus, it is worth looking at the Nandra et al. (1997) results critically. Table 3 in Nandra et al. (1997) reports the results of fits to 23 spectra from 18 Seyfert AGN. A single broad Gaussian was used to model Fe disk lines. But how many of these detections are robust? A modest requirement on the line width might be: $FWHM/err(FWHM) \geq 2$. Only eight sources pass this cut. This certainly does not mean that only 8 of 18

sources can be expected to have disk lines, on average. However, it does mean that as of 1997, *ASCA* observations had only yielded modestly convincing detections of relativistic disk lines in eight sources. The fact that the new survey detailed in Nandra et al. (2006) finds relativistic disk lines in 73% of Seyferts – though more conservative modeling is employed and an exposure criterion is enforced – strongly confirms that lines are commonly found in deep observations. This finding is supported by Guainazzi, Bianchi, & Dovciak (2006).

The results of the informal Seyfert census are given in Table 1. The number of strong disk line detections in Seyfert AGN is clearly *growing* in the *Chandra*, *XMM-Newton*, and *Suzaku* era. There are now nine sources with very strong disk line detections, a further six sources with compelling evidence for disk lines, and 15 sources with detections that need to be confirmed and investigated more deeply. If we take each of these detections at face value, then the 18 sources reported by Nandra et al. (1997) has increased to 30. Many prior detections with *ASCA* are confirmed and some new detections have been made. In a small number of cases, lines detected with *ASCA* are no longer detected. Given that line variability patterns prove to be complex, it is likely that some current non-detections are due to intrinsic variability. In some cases, prior detections with *ASCA* may have been erroneous.

The results of the informal census of stellar-mass black holes are given in Table 2. The ability to obtain moderate and high resolution spectra has transformed the field, bolstered prior claims based on gas detector spectra, and inspired new archival searches. Prior to *Chandra* and *XMM-Newton*, the line profile in Cygnus X-1 was likely the only case widely regarded as robust. In the current era, there are 16 sources in which compelling lines have been detected, of 19 in which lines could have been detected. Of eight sources observed well at CCD or gratings resolution, six show relativistic disk line profiles. Thus, relativistic lines are detected in 75–85% of stellar-mass black holes, in strong agreement with the detection fraction in Seyfert-1 AGN (Nandra et al. 1997; Nandra et al. 2006).

It is difficult to detect continuum emission or lines from the inner disk in Seyfert-2 AGN, due to obscuration from the torus. It is also difficult to detect relativistic disk lines in stellar-mass black holes that are viewed at high inclinations. While *Chandra* observations of XTE J1118+480 did not achieve the sensitivity required to detect or reject disk lines, sensitive observations have been made of other edge-on black holes. A disk line has never been convincingly detected in 4U 1630–472, and simultaneous *Chandra* and *RXTE* observations of H 1743–322 did not reveal disk line emission with tight limits (Miller et al. 2006b). There is likely no geometry in stellar-mass black holes that accurately mimics the torus, but obscuration from the outer accretion disk and/or enhanced scattering effects due to the edge-on viewing angle may act to limit our ability to detect disk lines.

7 Constraints on the Innermost Accretion Flow Geometry

The nature of hard X-ray emission in black holes is an outstanding problem. At present, it is not clear which process gives the dominant contribution to the observed X-ray emission. The geometry of the emitting region(s) is an closely related problem. A central Comptonizing “corona”, magnetic flaring loops above the disk, and processes in the base of a jet may all play a role. Indeed, these

possibilities may not even be distinct – they may all be related and part of a larger process. Relativistic disk lines and the larger disk reflection spectrum arise through the interaction of the hard X-ray region and the inner disk. As a result, these features can both serve to measure the inner disk radius and to constrain the nature of the hard X-ray emission region.

Recent disk line studies provide growing evidence that hard X-ray emission may be incredibly central and compact (somewhat arbitrarily, within $10 r_g$ or less), at least at reasonably high mass accretion rates (e.g., $L_X/L_{Edd} \geq 0.01$). Steep line emissivity profiles have now been measured in a number of Seyfert AGN and stellar-mass black holes (e.g., Wilms et al. 2001, Miller et al. 2002b), indicating strongly centralized energy dissipation. While this is consistent with a torque at the inner disk (perhaps through magnetic connections to the ergosphere or matter in the plunging region), the success of light bending models for X-ray variability suggests that a small source only a few r_g above the hole may provide much of the hard X-ray emission (e.g., Miniutti & Fabian 2004). In turn, this suggests that only a few flares (or perhaps the base of a jet) may dominate hard X-ray production in actively accreting black holes (Uttley & McHardy 2001, Uttley, McHardy, & Vaughan 2005; for a treatment of jets and coronae, see Markoff, Nowak, & Wilms 2005).

The variability seen in narrower components in the line profiles observed in NGC 3516 and Mrk 766 (Iwasawa, Miniutti, & Fabian 2004; Turner et al. 2006) is also consistent with relatively small magnetic flares. These observations suggest that flares need not be extremely centralized, and that flares can co-rotate above the disk for the duration of an orbit (or more). It is not clear if the line variability seen in these systems is plausibly consistent with variable reflection due to a warp, as may be the case in GRS 1915+105 (Miller & Homan 2005).

The nature of the innermost accretion flow at low accretion rates is also a matter of some uncertainty. Some models suggest that the innermost disk may radially recede, and be replaced by an advection-dominated inner flow. Recent analysis of relativistic disk line and continuum spectra from the stellar-mass black holes Cygnus X-1 and GX 339–4, and the black hole candidate SWIFT J1753.5–0127 in the “low/hard” state suggests that disks instead remain at or close to the ISCO for $L_X/L_{Edd} \geq 0.003$ (Miller et al. 2006b). Low-luminosity AGN like M81 and NGC 4258 offer the chance to study inner flow geometries at much lower fractions (roughly 100–1000 times lower) of the Eddington luminosity. The possibly relativistic line profile in M81 appears to be a collection of narrow lines, perhaps indicating that a thin disk does not extend to the ISCO (Dewangan et al. 2004). At present, differing results from analyses of the Fe line in NGC 4258 do not give a coherent picture of this source (Reynolds, Nowak, & Maloney 2000; Fruscione et al. 2005).

8 Summary and Future Prospects

Robust explorations and tests of exotic scientific predictions require well-understood tools that will serve to generate as many trials as possible. Whether exploring General Relativity, or how black holes and galaxies co-evolve, relativistic disk lines satisfy this criteria. Observations being made with current observatories show that the next generation of X-ray missions are poised to fulfill their enormous promise.

In recent years, the utility of relativistic disk lines has been tested and confirmed. Current observations clearly show that deep observations require relativistic disk lines in a high fraction of Seyfert-1 AGN, and the number of sources in which disk lines have been detected continues to grow. The fact that disk lines are observed in both supermassive and stellar-mass black holes facilitates many fundamental comparisons. Moreover, recent theoretical advances have kept pace: the recent development of variable-spin line models is ideally timed to coincide with the launch of *Suzaku*, and new deep *XMM-Newton* observations.

Thus, although spin constraints were possible in the past, realistic spin measurements are possible now, and it is essential that the field pursue such measurements in the next few years. Although many line profiles and variability trends strongly suggest high black hole spin parameters in a number of sources, this is only confirmed in the case of MCG-6-30-15 (Brenneman & Reynolds 2006). Deep *XMM-Newton* and *Suzaku* observations and systematic measurements of spin parameters are urgently needed. Long observations of Tier 2 and Tier 3 Seyferts, and of all new transient stellar-mass black holes, are required to build statistics.

There are already important indications that future missions like *Constellation-X* and *XEUS* will be able to measure spin in a large number of black holes, and to probe the spin history of AGN out to moderate red-shift. Streblyanska et al. (2005) examined deep *XMM-Newton* observations of the Lockman Hole; after adding the spectra of AGN in similar red-shift bins out to $z = 2$, relativistic disk lines are revealed in both the average Seyfert-1 and Seyfert-2 spectra (please see Figure 14). A separate analysis of *XMM-Newton* and *Chandra* deep fields reaches similar conclusions (Comastri, Brusa, & Gilli 2006). Current predictions suggest that 70% of all supermassive black holes should have maximal spin (Volonteri et al. 2005), and only missions such as *Constellation-X* and *XEUS* will be able to test such models and better our understanding of how black holes and galaxies co-evolve.

Quite apart from time-averaged measurements of spin, iron line “reverberation mapping” offers an excellent opportunity to probe strong-field gravitational effects (Reynolds et al. 1999, Young & Reynolds 2000). With sufficiently high collecting area, it becomes possible to watch the disk respond to individual hard X-ray flares through the evolution of iron line emission. The flux pattern observed (the “transfer function”) encodes precise information on the black hole spin and the nature of inner accretion flow. New results suggesting orbiting flares (e.g., Iwasawa, Miniutti, & Fabian 2004), gravitational light bending (e.g., Miniutti & Fabian 2004), and centrally-concentrated X-ray emission all bode extremely well for reverberation mapping. For a broad range of configurations, *Constellation-X* and *XEUS* will be able to perform reverberation mapping in approximately 10 Seyfert AGN in addition to the hundreds of spin determinations possible via fits to time-averaged line profiles.

Acknowledgments

I would like to thank all of my colleagues for their hard work in this area. I would especially like to acknowledge the following people for their comments and generosity: Andy Fabian, Jeroen Homan, Kazushi Iwasawa, Julian Krolik, Alex Markowitz, Giovanni Miniutti, Paul Nandra, Michal Nowak, James Reeves, Chris Reynolds, Jane Turner, and Simon Vaughan. Everyone active in this field is

indebted to Fred Jansen, Kazuhisa Mitsuda, Arvind Parmar, Norbert Schartel, Jean Swank, Harvey Tananbaum, and Nick White for directing missions (and planning future missions) that make this work possible.

References

- Agol E, Krolik JH, 2000. *Ap. J.* 528: 161–170
- Armitage PJ, Reynolds CS, 2003. *MNRAS* 341: 1041–1050
- Arnaud K, Branduardi-Raymont G, Culhane JL, et al., 1985. *MNRAS* 101: 17–20
- Arnaud K, 1996. *ADASS V*, ASP 216: 591–594
- Balestra I, Bianchi S, Matt G, 2004. *Astron. Astrophys.* 415: 437–442
- Ballantyne DR, Iwasawa K, Fabian AC, 2001. *MNRAS* 323: 506–516
- Ballantyne DR, Ross RR, Fabian AC, 2002. *MNRAS* 336: 867–872
- Balucinska-Church M, Church MJ, 2000. *MNRAS* 312: L55–59
- Bardeen JM, Press WH, Teukolsky SA, 1972. *Ap. J.* 178: 347–369
- Barr P, White NE, Page CG, 1985. *MNRAS* 216: 65–70
- Beckwith K, Done C, 2004. *MNRAS* 352: 353–362
- Blandford RD, Znajek RL, 1977. *MNRAS* 179: 433–456
- Branduardi-Raymont G, Sako M, Kahn SM, et al., 2001. *Astron. Astrophys.* 365: L140–145
- Brenneman LW, Reynolds CS, 2006. *Ap. J.* 652: 1028–1043
- Campana S, Stella S, Belloni T, et al., 2002. *Astron. Astrophys.* 384: 163–170
- Comastri A, Brusa M, Gilli R, 2006. In the proceedings of “Relativistic Astrophysics and Cosmology – Einstein’s Legacy”, ed. B Aschenbach, V Burwitz, G Hasinger, B Liebundgut, 7–11 November 2005, Munich, Germany
- Crummy J, Fabian AC, Gallo L, Ross RR, 2006. *MNRAS* 365: 1067–1081
- Cui W, Heindl WA, Swank JH, Smith D, Morgan EH, et al., 1997. *Ap. J.* 487: L73–76
- Dewangan GC, Griffiths RE, Schurch, NJ, 2003. *Ap.J.* 592: 52–61
- Dewangan GC, Griffiths RE, Di Matteo T, Schurch NJ, 2004. *Ap. J.* 607: 788–793
- Diaz Trigo M, Parmar AN, Miller JM, Kuulkers E, Caballero-Garcia, MD, 2006. *Astron. Astrophys.*, in press, astro-ph/0610873
- Done C, Zycki, PT, 1999. *MNRAS* 305: 457–468
- Done C, Gierlinski M, 2006. *MNRAS* 367: 659–668
- Dovciak M, Bianch S, Guainazzi M, Karas V, Matt G, 2004. *MNRAS* 350: 745–755
- Dovciak M, Karas V, Yaqoob T, 2004. *Ap. J. S.* 153: 205–221
- Ebisawa K, Ueda Y, Inoue H, Tanaka Y, White NE, 1996. *Ap. J.* 467: 419–434
- Fabian AC, Rees MJ, Stella L, White NE, 1989. *MNRAS* 238: 729–736
- Fabian AC, Vaughan S, Nandra K, Iwasawa K, Ballantyne RD, et al., 2002. *MNRAS* 335: L1–5
- Fabian AC, Miniutti G, Gallo L, Boller Th, Tanaka Y, et al., 2004. *MNRAS* 353: 1071–1077
- Fabian AC, Miniutti G, Iwasawa K, Ross RR, 2005. *MNRAS* 361: 795–802
- Fabian AC, Miniutti G, 2006. In “Kerr Spacetime: Rotating Black Holes in General Relativity”, ed. DL Wiltshire, M Visser, SM Scott, Cambridge University Press, Cambridge UK

- Fragile P, Miller WA, Vandernoot E, 2005. *Ap. J.* 635: 157–166
- Frank J, King A, Raine D., 2002. “Accretion Power in Astrophysics”, Third Edition, Cambridge University Press, Cambridge UK
- Fruscione A, Greenhill LJ, Filippenko AV, Moran JM, Herrnstein JR, et al., 2005. *Ap. J.* 624: 103–117
- Gallo LC, Boller Th, Brandt WN, Fabian AC, Vaughan S, 2004. *Astron. Astrophys.* 417: 29–38
- Gallo LC, 2006. *MNRAS* 368: 479–486
- George IM, Fabian AC, 1991. *MNRAS* 249: 352–367
- Gierlinski M, Done C, 2004. *MNRAS* 349: L7–11
- Gilfanov M, Churazov E, Revnivtsev M, 2000. *MNRAS* 316: 923–928
- Gondoin P, Orr A, Lumb D, Santos-Lleo M, 2002. *Astron. Astrophys.* 388: 74–87
- Guainazzi M, Matt G, Molendi S, Orr A, Fiore F, et al., 1999. *Astron. Astrophys* 341: L27–30
- Guaizazzi M, 2003. *Astron. Astrophys.* 401: 903–910
- Guainazzi M, Bianchi S, Dovciak M, 2006. *Astron. Nachr.* 327: 1032–1038
- Houck JC, Denicola LA, 2000. *ADASS IX*, ASP 216: 591–594 Iwasawa K, Fabian AC, Reynolds CS, Nandra K, Otani C, et al., 1996. *MNRAS* 232: 1038–1048
- Iwasawa K, Lee JC, Young AJ, Reynolds CS, Fabian, AC, 2004. *MNRAS* 347: 411–420
- Iwasawa K, Miniutti G, Fabian AC, 2004. *MNRAS* 355: 1073–1079
- Kaspi S, Brandt WN, George IM, Netzer H, Crenshaw D, et al., 2002. *Ap. J.* 574, 643–662
- Kinkhabwala AA, 2003. PhDT, Columbia University, publication number 3095588
- van der Klis M, 2006. “Rapid X-ray Variability”, in “Compact Stellar X-ray Sources”, ed. W Lewin, M van der Klis, Cambridge University Press, Cambridge
- Krolik JH, 1999. “Active Galactic Nuclei”, Princeton University Press, Princeton
- Krolik JH, Hawley JF, 2002. *Ap. J.* 573: 754–763
- Krolik JH, Hawley JF, Hirose S, 2005. *Ap. J.* 622: 1008–1023
- Laming JM, Titarchuk L, 2004. *Ap. J.* 615: L121–124
- Laor A, 1991. *Ap. J.* 376: 90–94
- Laurent P, Titarchuk L, 2007. *Ap. J.* in press
- Lee JC, Ogle P, Canizares CR, Marshall HL, Schulz NS, et al., 2001. *Ap. J.* 554: L13–17
- Liebert J, Bergeron P, Eisenstein D, Harris HC, Kleinman SJ, et al., 2004. *Ap. J.* 606: L147–149
- Liedahl DA, Torres, DF, 2005. *Can. J. Phys.* 83: 1177–1240
- Longinotti AL, Sim SA, Nandra K, Cappi M. 2007. *MNRAS* 374: 237–247
- Magdziarz P, Zdziarski AA, 1995. *MNRAS* 273: 837–848
- Markoff S, Nowak MA, Wilms J, 2005. *Ap. J.* 635: 1203–1216
- Markovic D, Lamb FK, 1998. *Ap.J.* 507: 316–326
- Markowitz A, Reeves JN, Serlemitsos P, Yaqoob T, Awaki H, et al., 2006. *Astron. Nachr.* 327: 1079–1086
- Markowitz A, Reeves J, Braito V, 2006. *Ap. J.* 646: 783–800
- Martocchia A, Matt G, Karas V, Belloni T, Feroci M, 2002. *Astron. Astrophys.*

387: 215–221

Martocchia A, Matt G, Belloni T, Feroci M, Karas V, et al., 2006. *Astron. Astrophys.* 448: 677–687

Mason KO, Branduardi-Raymont G, Ogle P, Page MJ, Pecharewicz EM, et al., 2003. *Ap. J.* 582: 95–104

Matt G, Guainazzi M, Perola GC, Fiore F, Nicastro F, et al., 2001. *Astron. Astrophys.* 377: L31–34

McClintock JE, Shafee R, Narayan R, Remillard RA, Davis SW, et al., 2006. *Ap. J.* 652: 518–539

Miller JM, Fox DW, Di Matteo T, Wijnands R, Belloni T, et al., 2001. *Ap. J.* 546: 1055–1067

Miller JM, Fabian AC, Wijnands R, Remillard RA, Wojdowski P, et al., 2002a. *Ap. J.* 578: 348–356

Miller JM, Fabian AC, Wijnands R, Reynolds CS, Ehle M., et al., 2002b. *Ap. J.* 570: L69–73

Miller JM, Marshall HL, Wijnands R, Di Matteo T, Fox DW, et al., 2003. *MNRAS* 338: 7–13

Miller JM, Raymond J, Fabian AC, Homan J, Nowak MA, et al., 2004a. *Ap. J.* 601: 450–465

Miller JM, Fabian AC, Reynolds CS, Nowak MA, Homan J, et al., 2004b. *Ap. J.* 606: L131–134

Miller JM, Homan J, 2005. *Ap. J.* 618: L107–110

Miller JM, 2006. *Astron. Nachr.* 327: 997–1003

Miller JM, Homan J, Steeghs D, Rupen M, Hunstead RW, et al., 2006a. *Ap. J.* 653: 525–535

Miller JM, Raymond J, Homan J, Fabian AC, Steeghs D, et al., 2006b. *Ap. J.* 646: 394–406

Miniutti G, Fabian AC, Goyder R, Lasenby AN, 2003. *MNRAS* 344: L22–26

Miniutti G, Fabian AC, 2004. *MNRAS* 349: 1435–1448

Miniutti G, Fabian AC, Miller JM, 2004. *MNRAS* 351: 466–472

Miniutti G, Fabian AC, 2006. *MNRAS* 366: 115–124

Miniutti G, Fabian AC, Anabuki N, Crummy J, Fukazawa Y, 2007. *PASJ* in press: astro-ph/0609521

Misra R, Kembhavi AK, 1998. *Ap. J.* 499: 205–208

Misra R, Sutaria KF, 1999. *Ap. J.* 517: 661–667

Nandra K, George IM, Mushotzky RF, Turner TJ, Yaqoob T, 1997. *Ap. J.* 477: 602–622

Nandra K, 2006. *MNRAS* 368: L62–66

Nandra K, O’Neill PM, George IPM, Reeves JM, Turner TJ, 2006. *Astron. Nachr.* 327: 1039–1042

Nayakshin S, Kallman TR, 2001. *Ap. J.* 546: 406–418

O’Brien PT, Page K, Reeves JN, Pounds K, Turner MJL, 2001. *MNRAS* 327: L37–41

Ogle PM, Mason KO, Page MJ, Salvi NJ, Cordova FA, et al., 2004. *Ap. J.* 606: 151–167

Onken CA, Peterson BM, Dietrich M, Robinson A, & Salamanca IM, 2003. *Ap. J.* 585: 121–127

Park SQ, Miller JM, McClintock JE, Remillard RA, Orosz JA, et al., 2004. *Ap. J.* 610: 378–389

Peterson BM, 2007. “An Introduction to Active Galactic Nuclei”, 1997.

- Cambridge University Press: Cambridge UK
- Petrucci PO, Henri G, Maraschi L, Ferrando P, Matt G, et al., 2002. *Astron. Astrophys.* 388: L5–8
- Petrucci PO, Ponti G, Matt G, Maraschi L, Malzac J, et al., 2006. *Astron. Nachr.* 327: 1043–1046
- Piconcelli E, Sanchez-Portal M, Guainazzi M, Martocchia A, Motch C, et al., 2006. *Astron. Astrophys.* 453: 839–846
- Ponti G, Cappi M, Dadina M, Malaguti G, 2004. *Astron. Astrophys.* 417: 451–459
- Ponti G, Miniutti G, Cappi M, Maraschi L, Fabian AC, 2006. *MNRAS* 368: 903–918
- Porquet D, Reeves JN, 2003. *Astron. Astrophys.* 408: 119–125
- Porquet D, Kaastra JS, Page KL, O’Brien PT, Ward MJ, et al., 2004. *Astron. Astrophys.* 413: 913–920
- Porquet D, 2006. *Astron. Astrophys.* 445: L5–L8
- Pounds KA, Reeves JN, Page KL, Edelson R, Matt G, et al., 2003a. *MNRAS* 341: 953–960
- Pounds KA, Reeves JN, King AR, Page KL, O’Brien PT, et al., 2003b. *MNRAS* 345: 705–713
- Pounds KA, Reeves JN, Page KL, O’Brien PT, 2004. *Ap. J.* 605: 670–676
- Reeves JN, Turner MJL, Pounds KA, O’Brien PT, Boller Th, et al., 2001. *Astron. Astrophys.* 365: L134–139
- Reeves JN, Nandra K, George I M, Pounds KA, Turner TJ, et al., 2004. *Ap. J.* 602: 648–658
- Reeves JN, Fabian AC, Kataoka J, Kunieda H, Markowitz A, et al., 2006. *Astron. Nachr.* 327: 1067–1070
- Reeves JN, Awaki H, Dewangan GC, Fabian AC, Fukazawa Y, et al., 2007. *PASJ* in press: astro-ph/0610434
- Remillard RA, McClintock JE, 2006. *Annu. Rev. Astron. Astrophys.* 44: 49–92
- Revnivtsev M, Gilanov M, Churazov E, 1998. *Astron. Astrophys.* 339: 483–488
- Revnivtsev M, Borozdin KN., Priedhorsky WC, Vikhlinin A, 2000. *Ap.J.* 530: 955–965
- Reynolds CS, 1997. *MNRAS* 86: 513–537
- Reynolds CS, Begelman MC, 1997. *Ap. J.* 487: L135–138
- Reynolds CS, Young AJ, Begelman MC, Fabian, AC, 1999. *Ap. J.* 514: 164–179
- Reynolds CS, Wilms J, 2000. *Ap. J.* 533: 821–825
- Reynolds CS, Nowak MA, 2003. *Phys. Rev.* 377: 389–466
- Reynolds CS, Nowak MA, Maloney PR, 2000. *Ap. J.* 540: 143–145
- Reynolds CS, Wilms J, Begelman MC, Staubert R, Kendziorra E, 2004. *MNRAS* 349: 1153–1166
- Ross RR, Fabian AC, Young AJ, 1999. *MNRAS* 306: 461–466
- Rossi S, Homan J, Miller JM, Belloni T, 2005. *MNRAS* 360: 763–768
- Ruszkowski M, Fabian AC, Ross RR, Iwasawa K, 2000. *MNRAS* 317: L11–15
- Sako M, Kahn SM, Bruanduardi-Raymont G, Kaastra JS, Brinkman AC, et al., 2003. *Ap. J.* 596: 114–128
- Sanchez-Fernandez C, Santos-Lleo M, in ’t Zand JJM, Gonzalez-Riestra R, Altieri B, et al., 2006. *Astron. Nachr.* 327: 1004–1007
- Schnittman JD, Homan J, Miller JM, 2006. *ApJ* 642: 420–426
- Shakura NI, Sunyaev RA, 1973. *Astron. Astrophys.* 24: 337–355

- Shih DC, Iwasawa K, Fabian, AC, 2002. *MNRAS* 333: 687–696
- Sobczak GJ, McClintock JE, Remillard RA, Cui W, Levin AM, et al., 2000. *Ap. J.* 544: 993–1015
- Streblyanska A, Hasinger G, Finoguenov A, Barcons X, Mateos S, et al., 2005. *Astron. Astrophys.* 432: 395–400
- Strohmayer T, 2001. *Ap. J.* 552: L49–53
- Tanaka Y, Nandra K, Fabian AC, Inoue H, Otani C, et al., 1995. *Nature* 375: 659–661
- Thorne KS, 1974. *Ap. J.* 191: 507–519
- Titarchuk L, Kazanas D, Becker PA, 2003. *Ap. J.* 598: 411–418
- Torok G, Abramowicz MA, Kluzniak W, Stuchlik Z, 2005. *Astron. Astrophys.* 436: 1–8
- Turler M, Chernyakova M, Courvoisier TJJ, Foellmi C, Aller MF, et al., 2006. *Astron. Astrophys.* 451: L1–4
- Turner AK, Fabian AC, Lee JC, Vaughan S, 2004. *MNRAS* 353: 319–328
- Turner TJ, Mushotzky RF, Yaqoob T, George IM, Snowden SL, et al., 2002. *Ap. J.* 574: L123–127
- Turner TJ, Reeves JN, Kraemer SB, 2004. *Ap. J.* 603: 62–66
- Turner TJ, Kraemer SB, George IM, Reeves JN, Botorff MC, 2005. *Ap. J.* 618: 155–166
- Turner TJ, Miller L, George IM, Reeves JN, 2006. *Astron. Astrophys.* 445: 59–67
- Uttley P, McHardy I, 2001. *MNRAS* 323: L26–30
- Uttley P, McHardy I, Vaughan S, 2005. *MNRAS* 359: 345–362
- Uttley P, Fuscione A, McHardy I, Lamer G, 2003. *Ap. J.* 595: 656–664
- Uttley P, Taylor, RD, McHardy IM, Page JM, Mason KO, et al., 2004. *MNRAS* 347: 1345–1356
- Vaughan S, Fabian AC, 2004. *MNRAS* 348: 1415–1438
- Vaughan S, Fabian AC, Ballantyne DR, De Rosa A, Piro L, et al., 2004. *MNRAS* 351: 193–205
- Volonteri M, Madau P, Quataert E, Rees, MJ, 2005. *Ap. J.* 620: 69–77
- Wang T, Lu Y, 2001. *Astron. Astrophys.* 377: 52–59
- Wilms J, Reynolds CS, Begelman MC, Reeves J, Molendi S, et al., 2001. *MNRAS* 328: L27–31
- van der Woerd H, White NE, Kahn SM, 1989. *Ap. J.* 344: 320–324
- Yaqoob T, George IM, Kallman TR, Padmanabhan U, Weaver KA, et al., 2003. *Ap. J.* 596: 85–104
- Yaqoob T, Reeves JN, Markowitz A, Serlemitsos PJ, Padmanabhan U, 2005. *Ap. J.* 627: 156–165
- Yaqoob T, Murphy KD, Griffiths RE, Haba Y, Inoue H, et al., 2007. *PASJ* in press: astro-ph/0609581
- Young AJ, Lee JC, Fabian AC, Reynolds CS, Gibson RR, et al., 2005. *Ap. J.* 631: 733–740
- Young AJ, Reynolds CS, 2000. *Ap. J.* 529: 101–108
- Young AJ, Ross RR, Fabian AC, 1998. *MNRAS* 300: L11–15
- in 't Zand JJM, Miller JM, Oosterbroek T, Parmar AN, 2002. *Astron. Astrophys.* 394: 553–560
- in 't Zand JJM, Markwardt CB, Bazzano A, Cocchi M, Cornelisse R, et al., 2002. *Astron. Astrophys.* 390: 597–609
- Zycki PT, Done C, Smith DA, 1999. *MNRAS* 305: 231–240

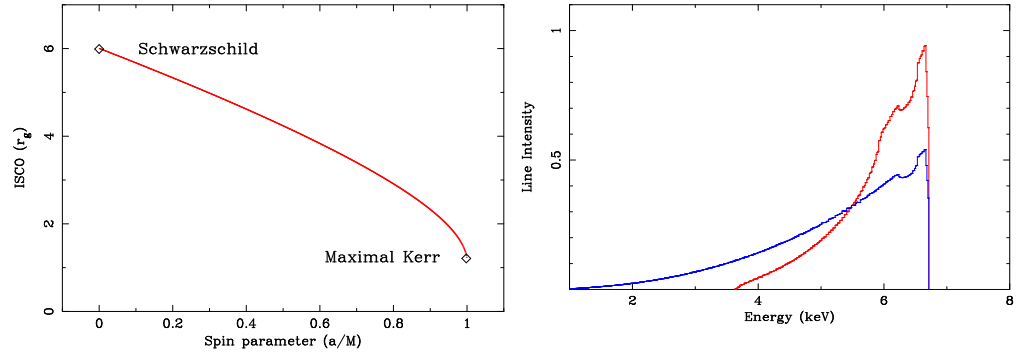


Figure 1: *Left*: The dependence of the innermost stable circular orbit (ISCO) on the black hole spin parameter is shown here, from Schwarzschild ($a = 0$) to maximal Kerr ($a = 0.998$) solutions. *Right*: The line profiles predicted in the case of Schwarzschild (red) and maximal Kerr (blue) black holes are shown here. It is the extent of the red wing and its importance relative to the blue wing that allow black hole spin to be determined with disk lines. (Adapted from Fabian & Miniutti 2006).

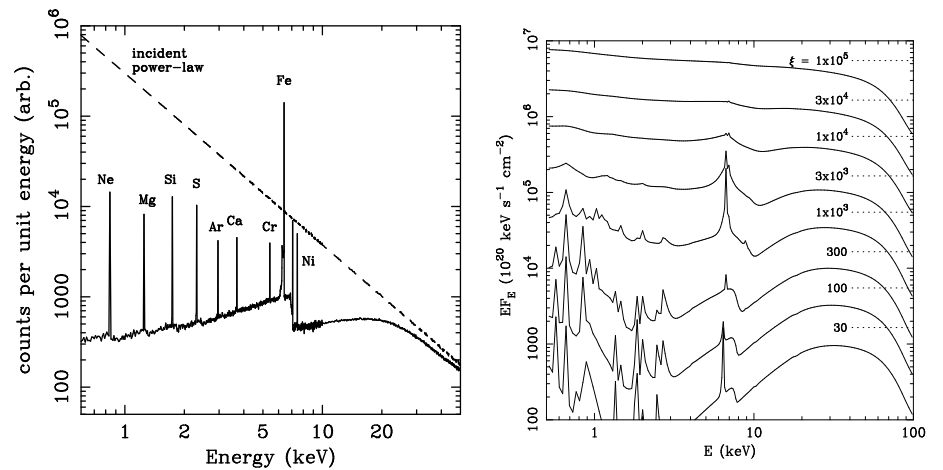


Figure 2: *Left*: The response of a neutral slab of gas to an incident power-law is shown here; this response spectrum is the disk reflection spectrum. (Adapted from Reynolds 1997). *Right*: The ionization of an accretion disk affects the reflection spectrum in predictable ways. Higher ionization results in greater broadening via scattering in the disk atmosphere. (Adapted from Ross, Fabian, & Young 1999.)

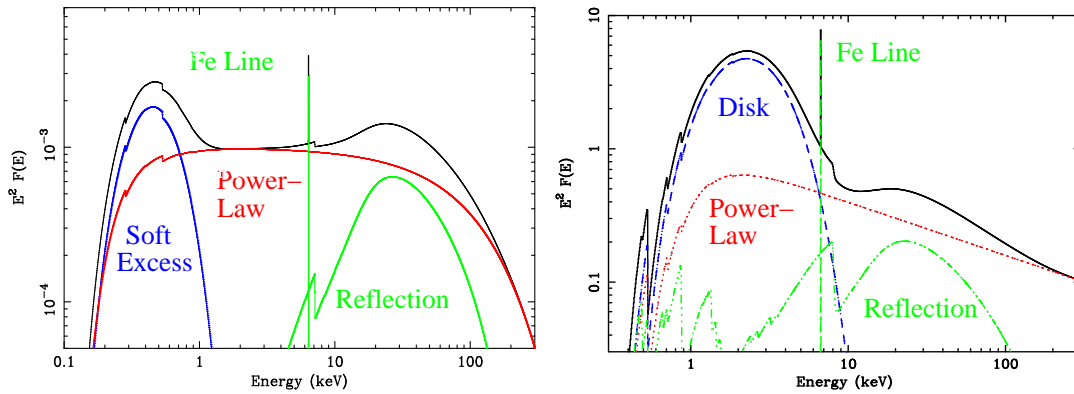


Figure 3: Representative continuum and disk response spectra for a Seyfert-1 AGN (left) and stellar-mass black hole (right) are shown above. The relativistic effects that shape the Fe line and reflection have not included, so the Fe line is narrow. In both cases, a power-law is chosen to model the hard X-ray emission, but the stellar-mass black hole power-law has a higher cut-off. The effect of neutral line-of-sight absorption in the Milky Way is also included in both cases. The “soft excess” component in the Seyfert-1 spectrum is shown here as a blackbody but may arise through disk reflection; please see the text for details. (The left panel is adapted from Fabian & Miniutti 2006.)

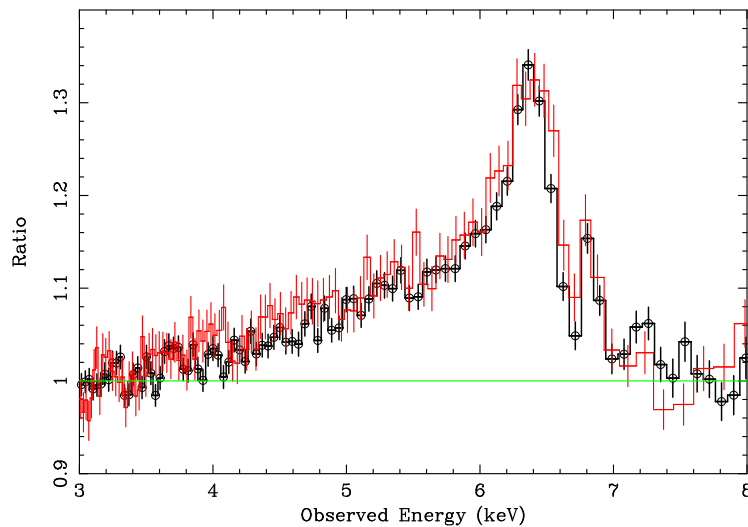


Figure 4: The figure above shows the relativistic disk line profile revealed in MCG-6-30-15 after fitting for the continuum. (Adapted from Miniutti et al. 2007 and Reeves et al. 2006.) The line in MCG-6-30-15 is the best example known presently, and these spectra above are the best yet obtained. The spectrum in black was obtained with *Suzaku*, and the spectrum in red was obtained with *XMM-Newton*.

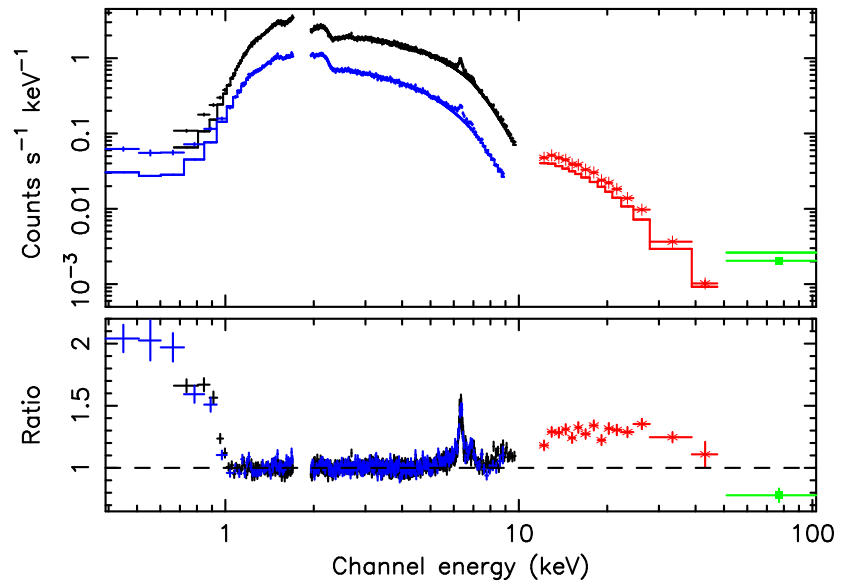


Figure 5: The figure above shows a *Suzaku* spectrum of the Seyfert-1 AGN MCG-5-23-16 fit with a simple absorbed power-law (Reeves et al. 2007). The ratio of the data to this model is shown in the lower panel. This figure demonstrates the ability of *Suzaku* to reveal all of the key features of Seyfert X-ray spectra simultaneously, including the soft excess, narrow iron line from distant reflection, and broad iron line and reflection from the inner disk. (The different colors merely reflect spectra obtained using different cameras. The figure was adapted from Reeves et al. 2007.)

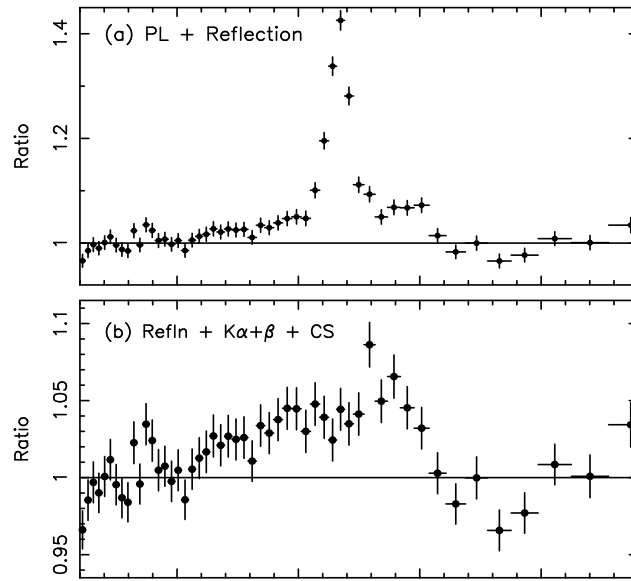


Figure 6: The figure above shows the data/model ratio resulting from more sophisticated fits to the spectrum of MCG-5-23-16 (Reeves et al. 2007). The top panel reveals narrow and broad Fe K lines after fitting for the continuum and disk reflection. The bottom panel shows the relativistic disk line that is revealed after fitting for narrow Fe K α and Fe K β lines. (The figures above are adapted from Reeves et al. 2007.)

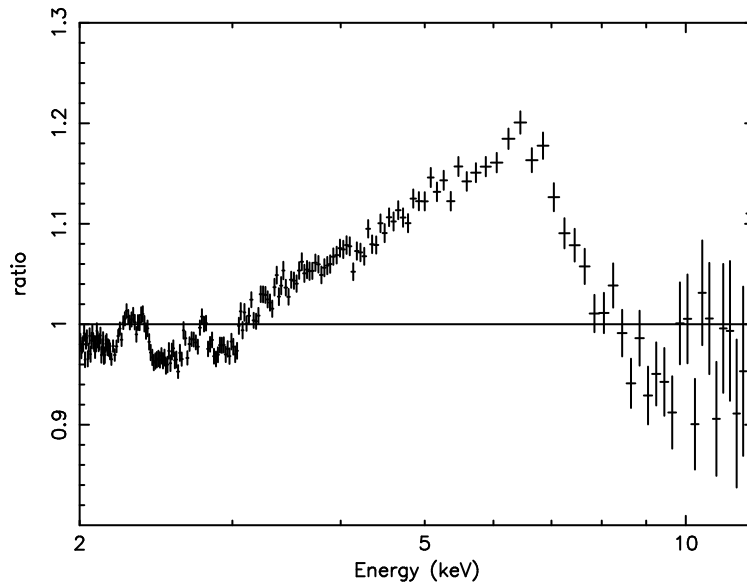


Figure 7: The relativistic Fe line revealed in an *XMM-Newton* spectrum of the stellar-mass black hole GX 339–4 in a “Very High” state is shown above. Fits with phenomenological and physical models suggest that GX 339–4 harbors a black hole with $a \geq 0.9$. (Adapted from Miller et al. 2004a). The red wing of the line profile seen above is extreme, and similar to that observed in MCG-6-30-15.

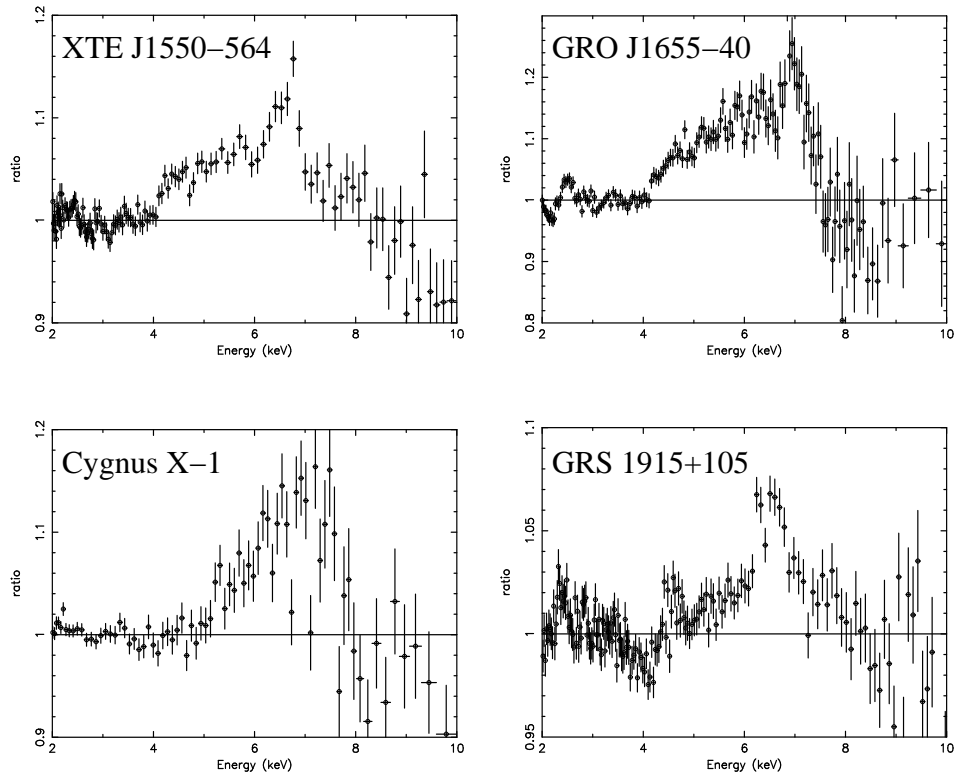


Figure 8: The figure above shows the relativistic disk line profiles revealed in an analysis of archival *ASCA*/*GIS* spectra of stellar-mass black holes that were observed in bright phases. (Adapted from Miller et al. 2005). The line profile in GRS 1915+105 is clearly not as skewed as the others, and does not strongly require black hole spin.

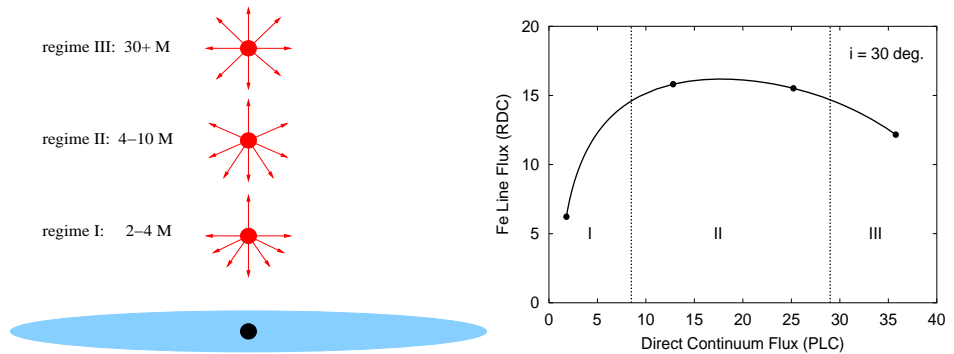


Figure 9: *Left*: This panel depicts the ability of gravitational light bending to focus emission from a constant-luminosity source at different source heights (above, $r = GM/c^2$, with $G = c = 1$, and the figure is not shown to scale). Close to the black hole, the source emission is far from isotropic. *Right*: Whereas a linear relation between Fe line flux and ionizing continuum flux is expected in the absence of light bending, a distinctly non-linear relation is expected when light bending is important, as shown in the panel on the right. (Adapted from Miniutti & Fabian 2004.) The regimes defined in this panel are depicted in the panel shown at left.

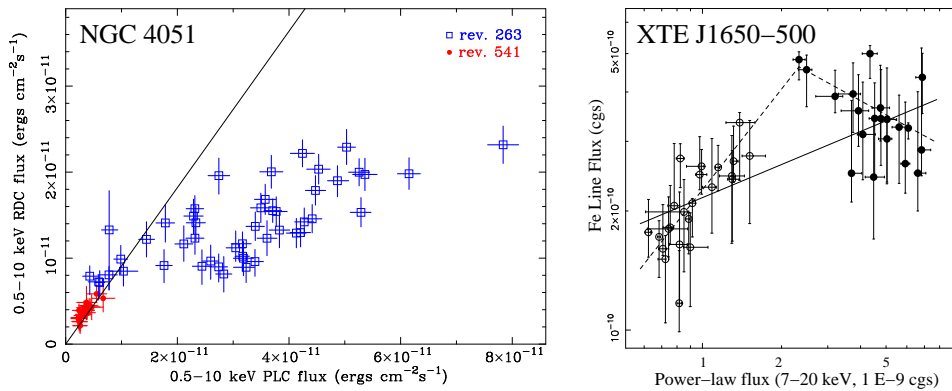


Figure 10: *Left*: The relationship between the flux in the disk reflection component and the irradiating power-law flux in the Seyfert-1 AGN NGC 4051 is shown here. (Adapted from Ponti et al. 2006.) *Right*: The relationship between Fe line flux and the disk-irradiating power-law flux in the stellar-mass black hole XTE J1650–500 is shown in this panel. (Adapted from Rossi et al. 2005.) In each case, it is clear that the line/reflection and power-law fluxes are directly related at low fluxes. The overall trends shown here are consistent with the flux relations predicted by models for gravitational light bending close to spinning black holes (e.g., Miniutti & Fabian 2004). A growing number of Seyfert AGN display similar trends; more work is needed in the case of stellar-mass black holes.

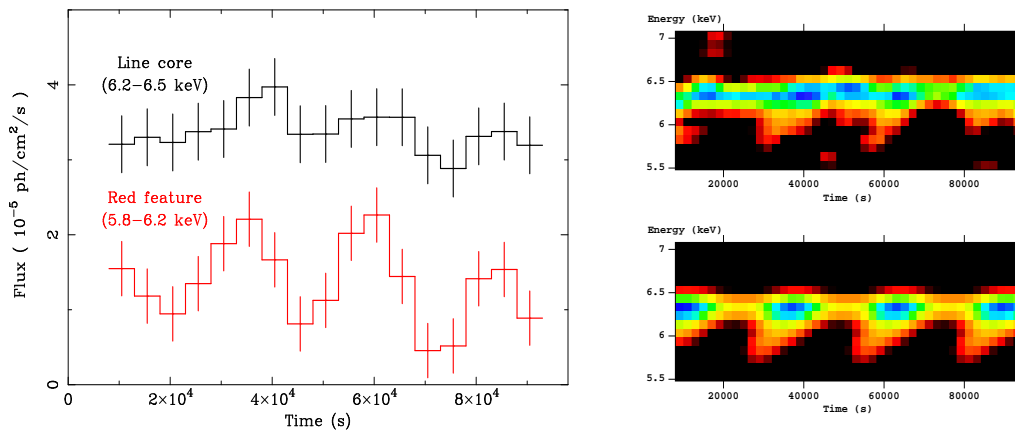


Figure 11: *Left*: The lightcurves of components in the Fe K band of NGC 3516 is shown here. One narrow line component in the Fe K band is especially variable. *Above right*: In this figure, the variations at left are shown as a trailed flux excess versus time map. *Below right*: A theoretical model for the Fe line flux variations based on a flare orbiting the black hole at radius of only 7–16 r_g is shown here (Iwasawa, Miniutti, & Fabian 2004; see also Fabian & Miniutti 2006). The sawtooth pattern is a direct result of the extreme environment close to the black hole. The remarkable similarity of the data and model suggests that observations of Seyferts with *XMM-Newton* and *Suzaku* can begin to probe orbital timescale variability. (The figures above were adapted from Iwasawa, Miniutti, & Fabian 2004.)

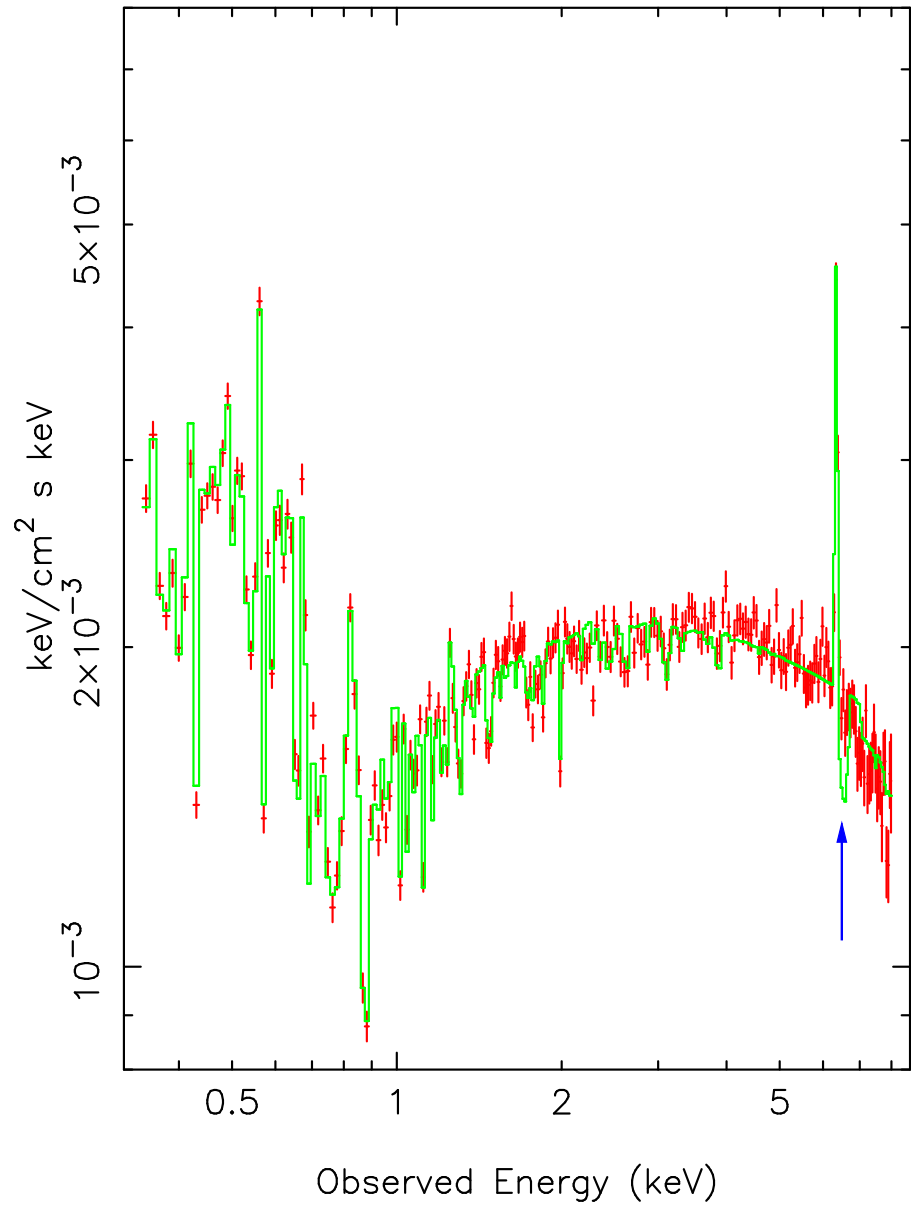


Figure 12: An *XMM-Newton* spectrum of Seyfert-1 AGN NGC 3516 is shown above, fit with a model including warm/hot absorption adding curvature to the Fe K band (Turner et al. 2004). The blue arrow emphasizes a low-ionization Fe absorption line predicted near to 6.4 keV that is not observed. As with MCG-6-30-15, this spectrum shows that relativistic lines, not absorption, must create the curvature observed in the Fe K band. (The figure above was adapted from Turner et al. 2004.)

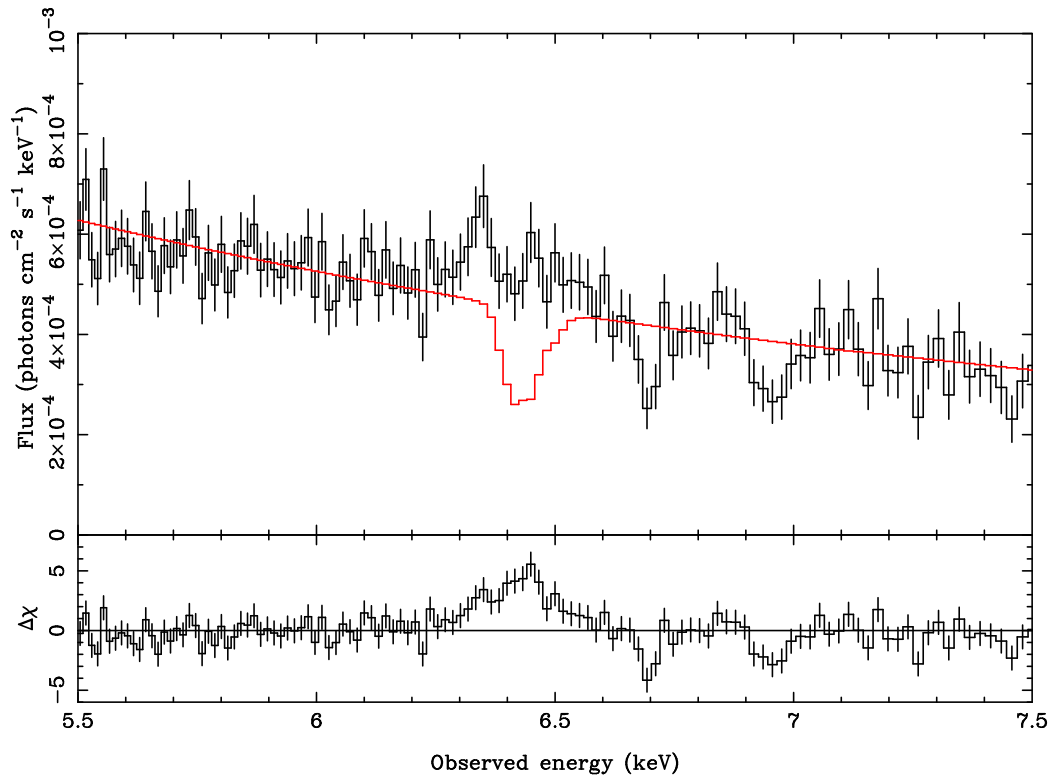


Figure 13: The 522 ksec *Chandra*/HETGS spectrum of MCG-6-30-15 is shown above, fit with a model that would explain curvature in the Fe K band as absorption rather than a relativistic line. The model predicts a strong neutral absorption which is not observed, signaling that curvature in the Fe K band is indeed due to relativistic disk lines in Seyfert AGN (Young et al. 2005). (The figure above was adapted from Young et al. 2005.)

Tier 1			
3C 120 ¹	NGC 2992 ²	MCG-5-23-16 ³	NGC 3516 ⁴
NGC 3783 ⁵	NGC 4051 ⁶	NGC 4151 ⁷	Mrk 766 ⁸
MCG-6-30-15 ⁹			
Tier 2			
Mrk 335 ¹⁰	Q 0056–363 ¹¹	IRAS 06269–0543 ¹²	PG 1425+267 ¹³
Mrk 841 ¹⁴	IRAS 18325–5926 ¹⁵		
Tier 3			
I Zw 1 ¹⁶	Fairall 9 ¹⁷	Mrk 359 ¹⁸	ESO 198-G24 ¹⁹
1H 0419-577 ²⁰	Ark 120 ²¹	MCG-02-14-009 ²²	1H 0707-495 ²³
PG 1211+143 ²⁴	Mrk 205 ²⁵	3C 273 ²⁶	4U 1344-60 ²⁷
IC 4329a ²⁸	NGC 5506 ²⁹	II Zw 177 ³⁰	

Table 1: Seyfert AGN in which relativistic disk lines have been detected are listed above. The sources are grouped into tiers according to the nature of the detections; please see the text for details. ¹ Reeves et al. (2006); ² Yaqoob et al. (2007), Reeves et al. (2006); ³ Reeves et al. (2006,2007); ⁴ Turner et al. (2002), Markowitz et al. (2006); ⁵ Nandra et al. (2006); ⁶ Nandra et al. (2006), Ponti et al. (2006), Reeves et al. (2006); ⁷ Nandra et al. (2006); ⁸ Mason et al. (2003), Nandra et al. (2006); ⁹ Wilms et al. (2001), Fabian et al. (2002); Reynolds et al. (2004); Vaughan & Fabian (2004); Miniutti et al. (2007); ¹⁰ Gondoin et al. (2002), Longinotti et al. (2007); ¹¹ Porquet & Reeves (2003); ¹² Gallo et al. (2007, in prep.); ¹³ Miniutti & Fabian (2006); ¹⁴ Petrucci et al. (2002, 2006); ¹⁵ Iwasawa et al. (2004); ¹⁶ Gallo et al. (2004); ¹⁷ Brenneman et al. (2007, in prep.); ¹⁸ O’Brien et al. (2001); ¹⁹ Porquet et al. (2004), simple independent analysis done for this review; ²⁰ Pounds et al. (2004), Fabian et al. (2005); ²¹ Vaughan et al. (2004); ²² Porquet (2006); ²³ Fabian et al. (2004); ²⁴ Pounds et al. (2003); ²⁵ Reeves et al. (2001); ²⁶ Turler et al. (2006); ²⁷ Piconcelli et al. (2006); ²⁸ Markowitz, Reeves, & Braitto (2006); ²⁹ Matt et al. (2001); ³⁰ Gallo (2006).

Tier 1			
XTE J1550-564 ¹	XTE J1650-500 ²	GRO J1655-40 ³	GX 339-4 ⁴
SAX J1711.6-3808 ⁵	GRS 1915+105 ⁶	Cygnus X-1 ⁷	
Tier 2			
4U 1543-475 ⁸	V4641 Sgr ⁹	4U 1908+09 ¹⁰	XTE J2012+38 ¹¹
Tier 3			
GS 1354-64 ¹²	GRS 1737-31 ¹³	XTE J1748-28 ¹⁴	XTE J1755-32 ¹⁵
XTE J1859+226 ¹⁶			
Significant Non-Detections			
4U 1630-472	H 1743-322	SW J1753.5-0127	

Table 2: Stellar-mass black holes in which relativistic disk lines and sources with significant non-detections are listed above. The sources are grouped into tiers according to the nature of the line detections; please see the text for details. ¹ Miller et al. (2003,2004), Sobczak et al. (2000); ² Miller et al. (2004), Miniutti, Fabian, & Miller (2004); ³ Miller et al. (2004), Diaz Trigo et al. (2006); ⁴ Miller et al. (2004,2004,2006); ⁵ Martocchia et al. (2002,2006), Miller et al. (2004); ⁶ in 't Zand et al. (2002a), Sanchez-Fernandez et al. (2006); ⁷ Miller et al. (2002,2006); ⁸ Park et al. (2004), van der Woerd, White, & Kahn (1989); ⁹ Miller et al. (2002); ¹⁰ in 't Zand et al. (2002b); ¹¹ Campana et al. (2002); ¹² Revnivtsev et al. (2000); ¹³ Cui et al. (1997); ¹⁴ Miller et al. (2001); ¹⁵ Revnivtsev, Gilfanov, & Churazov (1998); ¹⁶ simple independent analysis done for this review; ¹⁷ numerous sources; ¹⁸ Miller et al. (2006); ¹⁹ Miller, Homan, & Miniutti (2006).

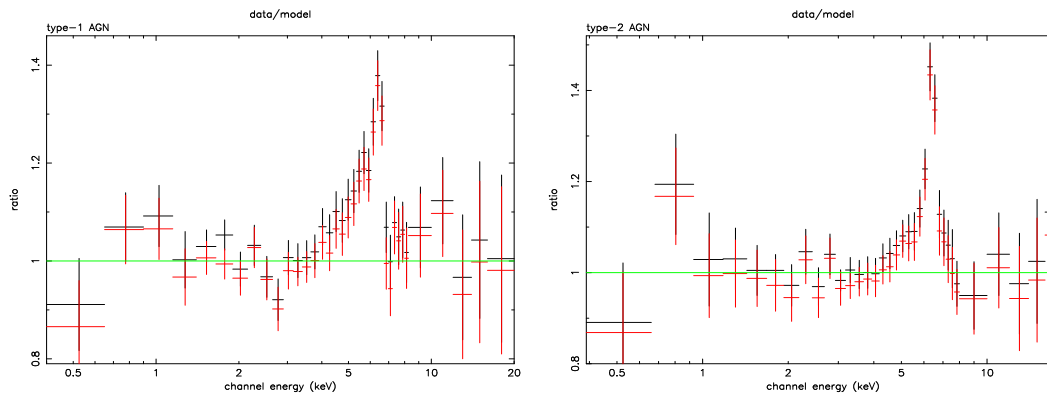


Figure 14: Relativistic disk-line profiles are revealed in spectrum of distant Seyfert-1 (left) and Seyfert-2 (right) AGN in a deep observation of the Lockman Hole made with *XMM-Newton* (Streblyanska et al. 2005). Individual spectra from sources out to $z \simeq 2$ were corrected to the rest frame and added to make the spectra above. This result makes it clear that future missions like *Constellation-X* and *XEUS* will be able to study the spin history of supermassive black holes. (The different colors above merely reflect spectra obtained with different cameras. This figure was adapted from Streblyanska et al. 2005.)